Organic & Biomolecular Chemistry

Accepted Manuscript

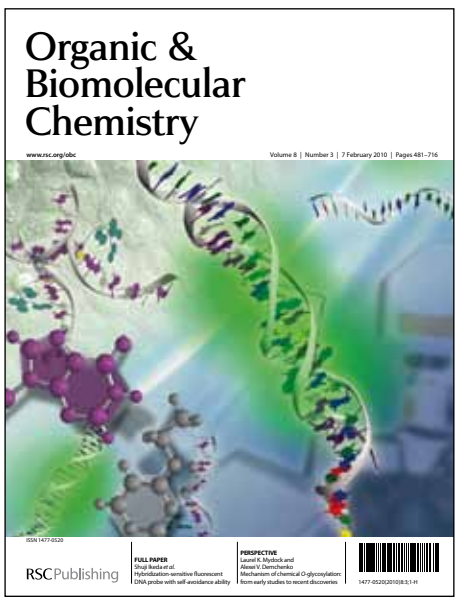

This is an *Accepted Manuscript*, which has been through the RSC Publishing peer review process and has been accepted for publication.

Accepted Manuscripts are published online shortly after acceptance, which is prior to technical editing, formatting and proof reading. This free service from RSC Publishing allows authors to make their results available to the community, in citable form, before publication of the edited article. This *Accepted Manuscript* will be replaced by the edited and formatted *Advance Article* as soon as this is available.

To cite this manuscript please use its permanent Digital Object Identifier (DOI®), which is identical for all formats of publication.

More information about *Accepted Manuscripts* can be found in the **Information for Authors**.

Please note that technical editing may introduce minor changes to the text and/or graphics contained in the manuscript submitted by the author(s) which may alter content, and that the standard **Terms & Conditions** and the **ethical guidelines** that apply to the journal are still applicable. In no event shall the RSC be held responsible for any errors or omissions in these *Accepted Manuscript* manuscripts or any consequences arising from the use of any information contained in them.

Organic & Biomolecular Chemistry

New model of binding of rifampicin and its amino analogues as zwitterions to bacterial RNA polymerase

Krystian Pyta,[a] Katarzyna Klich,[a] Piotr Przybylski*[a] and Joanna Stefańska[b]

[a]*Faculty of Chemistry, A. Mickiewicz University, Grunwaldzka 6, 60-780 Poznan, Poland*

[b]*Medical University of Warsaw, Department of Pharmaceutical Microbiology, Oczki 3, 02-007 Warsaw, Poland*

[*]*E-mail: piotrp@amu.edu.pl, tel. +48 61 8291252, fax. +48 61 829 1505*

Seven new benzyl (**3-9**) and four new phenethyl (**10-13**) amino analogues of *ansa*-macrolide rifampicin (**1**) were synthesized using the optimised method of reductive amination. Structures of **3-13** in solution were determined by 1D and 2D NMR and FT-IR methods whereas the energetically most favoured conformation of amino analogues was calculated with the use of PM5 method. Spectroscopic and semi-empirical studies revealed the presence of zwitterionic forms of all **3-13** analogues in solutions containing water traces. ^{1}H-^{15}N HSQC and ^{1}H-^{15}N HMBC in combination with ^{1}H-^{1}H COSY and ^{1}H-^{13}C HMBC two dimensional spectroscopic methods unambiguously evidenced that the presence of the zwitterionic form of *ansa*-macrolides was a consequence of proton transfer from O(8)-H phenolic group to secondary amine moiety within **3-13** structures. ^{1}H-^{1}H NOESY studies indicated two different orientations of the substituent introduced at C(3) position for benzyl and phenethyl amino analogues of rifampicin and their similar conformation within the *ansa*-bridges in solution. FT-IR studies of the deprotonation of molecule **1** and comparison of these data with those for **3-13** indicated C(8)=O double bond character after formation of zwitterions in solution. Results of antibacterial test against Gram-(-) and Gram-(+) strains were compared with detailed structural information on new analogues of **3-13** to indicate some structure-activity relationships. Molecular recognition studies of **1** and **12** inhibitors at the binding site of bacterial RNA polymerase (RNAP) as zwitterions revealed key intermolecular interactions and led to proposition of a new model of

RNAP inhibition, which explains significant differences in antibacterial properties of rifampicin and its analogues.

Keywords: rifampicin analogues; *ansa* macrolides; antibiotics; zwitterions; reductive amination; ^{1}H, ^{13}C and ^{15}N NMR, ^{1}H-^{1}H NOESY; FT-IR; antibacterial activity; bacterial RNA polymerase inhibitors.

Introduction

Rifampicin (Fig. 1), called in US rifampin, belongs to *ansa* macrolide group of antibiotics, characterised by strong antibacterial properties against Gram-positive and Gram-negative bacteria strains.[1] Because of relatively fast resistance of bacteria to this antibiotic, rifampicin is mainly used as therapeutic agent in combinatorial therapy against *tuberculosis* together with e.g. isoniazid and vancomycin.[2] Resistance of bacteria strains to rifampicin is mainly achieved *via* hydrolysis of hydrazone moiety at C(38) atom and glycosylation of hydroxyl groups of the *ansa* bridge or is gained by RNA polymerase (RNAP) mutations.[3] At the beginning the mechanism of rifampicin activity was supposed to depend on the allosteric inhibition of RNA polymerase.[4] Since the X-ray structure of rifampicin-RNA polymerase has been determined, it has been known that this mechanism is based on direct blocking of the elongated RNA transcript path at 5' end.[5] Although the problem of inhibitor binding site to RNA polymerase has been solved, the low accurancy of X-ray measurements of rifampicin has not allowed drawing conclusions on the types of interaction between the inhibitor molecule and the enzyme. Earlier studies also indicated that the arrangement of O(21)H and O(23)H hydroxyls of ansamycin bridge relative to naphthalene moiety in the rifamycin group of antibiotics influences their antibacterial activity.[6] Up to now a series of oxime, hydrazone, semicarbazone, iminium derivatives undergoing cyclisation processes and obtained *via* Wittig reaction at C(38) atom have been synthesised as potential alternative antibacterial agents to rifampicin.[7] Simple amino analogues of rifampicin at C(3), containing at nitrogen methyl, ethyl or propyl groups have also been obtained but not studied toward antibacterial activity against standard bacteria strains.[8] Recently, we have demonstrated that the protonation site of rifampicin-based antibiotics has strong impact on their antibacterial activity.[9] Taking into account that hydrolysis of hydrazone moiety at C(38) atom is one of the processes leading to bacteria resistance to rifampicin, to get more information about the character of the substituent at C(38) atom desired to achieve high antibacterial activity we

synthesised and biologically tested a new series of rifampicin amino analogues at C(38) atom, resistant to hydrolysis process, and containing various substituted phenyl ring with halogen. Recent reinvestigation of the X-ray structure of rifampicin pentahydrate[10] questioned the correctness of the model proposed by Darst et al.[5] of binding of rifampicin to bacterial RNA polymerase formulated on the basis of rifampicin pentahydrate structure[11] presented in the incorrect non-ionic form. Furthermore, the non-ionic structure of rifampicin was further used for molecular dynamics calculations of rifampicin and RNAP interactions.[12] Earlier we have demonstrated that formation of important for biological activity strong intermolecular hydrogen bond between E_{445} and protonated piperazine nitrogen atom of rifampicin is possible.[9] To get more insight into the molecular mechanism of inhibition of this important enzyme, the total optimisation of interactions between the inhibitor (compounds **1** and **12**) and the enzyme (bacterial RNA polymerase) at the semi-empirical level of theory has been performed with the use of PM5 method.

Results and discussion

Synthesis of new rifampicin amino analogues 3-13

Rifampicin was hydrolyzed into rifaldehyde and next converted into its new benzyl and phenethyl amino analogues (Fig. 2) *via* four the reductive amination methods (Fig. 1, Table 1). New amino analogues of rifampicin were characterised by 1D and 2D NMR, FT-IR and MALDI-TOF MS methods (see Experimental section, Figures 4 and 7). As shown in Table 1, application of $NaBH_4$ as reductant leads to the lowest yield, whereas the use of $NaBH_3CN$ in the presence of HCl/EtOH as a catalyst is shown to be the most efficient method. It should be emphasised that the use of cyanoborohydride on polymer support (method 4) as a reductant is not as efficient as the use of $NaBH_3CN$ (method 3), because of the absorption processes of rifaldehyde and respective rifampicin amino analogues on molecular sieves. Reductive amination *via* the application of a relatively "soft" reductant as $NaBH(CH_3COO)_3$ in the presence of HCl/EtOH was also a good choice comparing the yields of methods 2 and 3.

Structure of new rifampicin amino analogues 3-13 in solution

Earlier, on the basis of our X-ray and NMR studies, the intramolecular proton transfer process for **1** structure was indicated.[9] FT-IR spectra of **1** and **8** in aprotic and protic systems,

with the detailed assignment of the bands on the basis of deuteration, are presented in Figures 3a and b. Comparison of the spectra of **1** (Fig. 3a) in two different solvents and after addition of stoichiometric amount of KOH reveals important changes in the ν(C=O) and ν(C=C) band regions. In the FT-IR spectrum of **1** in $CHCl_3$ in the stretching vibration region characteristic of carbonyl group, three bands at 1715, 1660 and 1646 cm^{-1} appear assigned to $\nu(C_{35}=O)$ of acetate, $\nu(C_{11}=O)$ of ketone and $\nu(C_{15}=O)$ of amide group, respectively. The presence of these bands at these frequencies demonstrates that in $CHCl_3$ **1** exists exclusively in the non-ionic form (Fig. 2), which is in agreement with the previously obtained NMR data for **1** in $CHCl_3$.[9] Strong changes in FT-IR spectrum are observed upon addition of KOH to **1** in equimolar ratio (Fig. 2). The most spectacular difference is the appearance of bands at 1655, 1584, 1478 and 1476 cm^{-1}. A slight shift toward lower frequencies and a significant increase in the band absorption at 1655 cm^{-1} are evoked by deprotonation of the most acidic phenolic group at C(8) and formation of phenolate anion of **1** in $CHCl_3$ solution. The overlapping of $\nu(C_{11}=O)$ and $\nu(C_8=O)$ bands in the spectrum, indicates that the electron density of oxygen atom of C(8)-O^- phenolate group is strongly shared with the naphthalene ring and therefore at C(8) and C(11) positions two carbonyl groups are present. NMR spectra of deprotonated **1**, recorded in $CDCl_3$, are given in Figure 4. In the ^{13}C NMR spectrum of deprotonated **1** (Fig. 4b) there are two signals at 183. 2 and 188.6 ppm. Assignment of these signals, on the basis of 2D NMR spectra, to δ_{C8} and δ_{C11} resonances, confirms a similar character of $C_{11}=O$ and $C_8=O$ bonds. The increased electron density in the naphthalene ring, as a consequence of the proton transfer, influences also the position of ν(C=C) naphthalene skeleton vibrations i.e. two new bands of ν(C=C) from naphthalene ring appear at 1502 and 1476 cm^{-1}. It should be noted that as a result of the strong resonance effect also the ν(C=N) band shifts from 1567 to 1584 cm^{-1} toward higher frequencies revealing more double C=N bond character of hydrazone moiety. The appearance of $\nu(C_{35}=O)$ vibrations as two separate bands at 1719 and 1713 cm^{-1} can be explained by the conformational equilibrium of *ansa* bridge and bonding of acetate carbonyl group with O(23)H hydroxyl with different strength. The FT-IR spectrum of **1** in $DMSO/H_2O$ seems to be very similar to the respective spectrum of **1** in $CHCl_3$, recorded after addition of KOH, in 1800-1450 cm^{-1} analytical range. The presence of a characteristic band at 1655 cm^{-1} assigned to $\nu(C_{11}=O)$ and $\nu(C_8=O)$ vibrations along with bands at 1511 and 1478 cm^{-1} assigned to ν(C=C) naphthalene ring vibrations confirms the formation of zwitterionic form of **1** in $DMSO/H_2O$, in which our antibacterial tests have been performed.

Similar double character of C(8)=O and C(11)=O bonds for **1** is manifested by similar chemical shifts of δ_{C8} (184.2 ppm) and δ_{C11} (184.5 ppm) in DMSO-d_6/H_2O. In the FT-IR spectra of rifampicin analogues **3-13** (Fig. 3b) the above discussed bands, characteristic of zwitterionic form, also are found in the 1800-1450 cm^{-1} region, irrespectively whether recorded in $CHCl_3$ or DMSO/H_2O. Thus, as a consequence of intramolecular proton transfer process and resonance phenomenon for rifampicin analogues **3-13** the double character of C(8)-O bond is predominant in solution. This conclusion is supported by similar δ_{C8} values for **1** and **3-13** amino analogues in different solvents: in DMSO-d_6/H_2O (184.1-184.2 ppm) and in $CDCl_3$ (181.7-183.0 ppm[9]). The C(8)=O and C(11)=O bond parameters in the calculated structures of **8** and **12** (Fig. 5) support a similar character of these bonds because C(8)=O and C(11)=O bond length parameters are almost the same for **8** and for **12**, of 1.24 Å and 1.23 Å, respectively.

Localisation of the transferred proton in **1** in DMSO/H_2O has been established earlier as the tertiary nitrogen atom of the piperazine ring.[9] Essential information about the localisation of the transferred proton of O(8)-H group in the new rifampicin analogues **3-13** is provided by the 2D NMR spectra (Fig. 6). One bond ^1H-^{15}N couplings of the two protons giving signals at 9.20 and 8.56 ppm together with the ^1H-^1H spin-spin couplings of the same protons through three bonds with H(38) and H(39) protons reveal unambiguously that in **3-13** analogues the proton from O(8)-H group is at the secondary nitrogen atom N(38). Furthermore, chemical shifts of N(38) signals in ^{15}N NMR spectra of **3-13** are in a narrow range from -329 to -334 ppm (see Experimental section), typical of protonated amines.[13] The ^1H NMR chemical shifts of the two geminal (38)N^+-H protons are different (Fig. 7) because of the fact that these protons are diastereotopic due to the chirality of the molecule combined with the prochiral quaternary nitrogen center[14] and different character of hydrogen bonds in which these protons are involved. As shown in Figure 5, one of the protons, localised at the positively charged nitrogen atom, is engaged in a weak intramolecular hydrogen bond with the oxygen atom of amide group (length ~2.9 Å, angle ~150°), whereas the second one is intermolecularly bonded to solvent molecules. Zwitterionic form of **3-13** compounds is also well reflected in deshielding of the proton signal of O(1)-H hydroxyl group by about 3 ppm ($\delta_{O(1)\text{-}H}$ = 16.01-16.05 ppm) relative to its position in the spectrum of non-ionic form of **1** $\delta_{O(1)\text{-}H}$ = 13.19 ppm.[9] This spectral difference is a result of formation of a stronger O(1)-H···O=C(8) hydrogen bond (length ~2.5 Å, ~150°, Fig. 5) in a six membered system in zwitterions of **3-13** than the respective one O(1)-H ··· O=C(15) in a seven-

membered system, assumed by the non-ionic form of **1** in solution. The signal assigned to the phenolic group O(4)-H is found in the range 12.82-12.86 ppm in the spectra of **3-13** and its position indicates participation of this hydroxyl in intramolecular (11)O···H-O(4) hydrogen bond (length ~2.6 Å, angle ~178°, Fig. 5).

The orientation of *ansa* bridge relative to the naphthalene ring, which strongly contributes to biological activity, in structures of new derivatives **3-13** in DMSO-d_6 solution was determined on the basis of ^{1}H-^{1}H NOESY contacts (Fig. 8). Strong contacts between H(34) and H(14) protons of methyl groups for all derivatives clearly indicate the close vicinity of these groups and suggests the orientation of *ansa* bridge relative to naphthalene moiety as in the calculated structure shown in Figure 8a [distance H(34) ··· H(14) is 4 Å]. Furthermore, a strong shielding of H(34) signal to about -0.3 ppm in all ^{1}H NMR spectra of **3-13** is a result of the location of H(34) protons over the naphthalene ring π electron cloud. The spatial contacts of H(33) proton with the H(18) and H(38) protons, determined from ^{1}H-^{1}H NOESY spectra [distances: H(33) ··· H(18) is 3.8 Å; H(33) ··· H(38) is 2.5 Å], confirm the conformation of *ansa* bridge in solution as presented in Figure 8.

It should be noted that for **3-13** analogues there are several possible combinations of different C(16)=C(17) and C(18)=C(19) double bond configurations with different conformations of diene moiety (s-*cis* and s-*trans*). Assignment of H(18) and H(19) proton signals with the use of ^{1}H-^{13}C HSQC and ^{1}H-^{13}C HMBC methods and determination of three-bond coupling constants $^3J_{H18\text{-}H19}$≈15.5 Hz and $^3J_{H19\text{-}H20}$≈7.5 Hz for **3-13** compounds evidenced the *E*- configuration of C(18)=C(19) bond. The signal at 6.55 ppm assigned to H(18) proton is a double of doublets with one coupling constant as mentioned earlier and the other $^3J_{H18\text{-}H17}$=10.8 Hz, characteristic of s-*trans* conformation of diene moiety.[15] The determination of C(16)=C(17) bond configuration on the basis of one-dimmensional NMR spectra was difficult because of the absence of proton at C(16) atom. Instead, the ^{1}H-^{1}H NOESY spectra were found to be more informative and revealed that the resonance at 2.08 ppm of H(30) protons strongly correlates with H(17) and weakly with H(18) signals. This situation is well reflected in the following distances: H(30)···H(17) 2.31Å and H(30)···H(18) 4.56 Å, determined for all calculated structures (Fig. 8), in which *Z*- configuration of C(16)=C(17) is energetically favoured. Indirect evidence of C(16)=C(17) bond configuration as *Z*- are proton-proton contacts of H(18) with H(38), H(21) and N(2)-H protons (Fig. 8b), which

should not be observed if the double bond assumed the *E*- configuration in **3-13** structures. It is worth adding that $^{3}J_{H28\text{-}H29}$ close to 13 Hz indicates the *E*- configuration of C(28)=C(29) double bond.

Comparison of ^{1}H NMR resonances of diene moiety for **1** as well as benzyl (compounds **3-9**) and phenethyl (compounds **10-13**) amino derivatives (Fig. 7) indicates that different intramolecular interactions stabilize the structures of **1** and **3-13** in solution. Significant difference in δ_{H18} values between **1** and **3-13** is a result of different orientation of O=C(15)-N(2)-H amide group in **1** [intramolecular N(2)-H···N=C(38) bond] and in **3-13** [intramolecular C(15)=O···H-$^{+}$N(38) bond] structures and changes within the diene fragment conformation. Interesting are also the differences in $\delta_{H17,}$ δ_{H18} and δ_{H19} chemical shifts between **3-9** and **10-13** spectra indicating that for **10-13** the π-π stacking interaction between the electrons of diene with those of phenyl ring takes place. This difference is probably due to different lengths of the linker in phenethyl (-CH_2-CH_2-) and benzyl (-CH_2-) derivatives (Fig. 5). The π-π stacking interaction also weakens the intramolecular hydrogen bond C(15)=O···H-$^{+}$N(38) in the structure of **10-13** in solution, which is manifested by lower δ_{N+H} values, if compared to those recorded for **3-9** (Fig. 7, Experimental section).

Antimicrobial activity of 1 and 3-13 macrolides

Rifampicin (**1**) and a series of its amino analogues (**3-13**) containing benzyl and phenethyl moieties substituted with halogen were tested *in vitro* for their antibacterial properties against standard bacteria strains. The results collected in Table 2 demonstrate that all compounds studied are significantly more active against Gram-(+) than Gram-(-) negative bacteria strains. Newly synthesised benzyl amino analogues comprising fluorine atom at *o*- and *m*- positions (compounds **4** and **5**) are characterised by moderate antibacterial activity against two Gram-(-) negative strains *E. coli* (MIC = 64 μg/ml). The other amino analogues are rather less active or inactive against Gram-(-) bacteria strains. Generally, lower activity of **3-13** against Gram-(-) strains in comparison to that of **1** can be explained by structural differences of the substituent at C(3) position and different orientation of amide moiety resulting in lower lipophilicity and weaker penetration of Gram-(-) bacteria membranes. Rifampicin shows high antibacterial activity (MIC = 0.004-0.016 μg/ml) against Gram-(+) strains. The antibacterial activity of **3-13** amino analogues is lower (MIC = 0.125-4 μg/ml) than that of **1** against Gram-(+) bacteria strains but

comparable with that determined earlier (MIC = 0.125-0.5 μg/ml)[16] for another antibacterial agent - ciprofloxacin, a member of fluoroquinolones group, widely used for treatment of a number of infections.[17] The lowest activity against Gram-(+) strains is shown by compounds **3-13** against *S. aureus* ATCC 25923 strain, similarly as by **1**. Almost all of **3-13** compounds, reveal a very interesting high activity against both *S. epidermidis* ATCC 12228 and ATCC 35984 bacteria strains (MIC equal 0.5, 0.25 or 0.125 μg/ml), belonging to a group of bacteria evoking the infections accompanying insertion of plastic elements in the body, e.g. heart valves, medical prostheses. Combined analysis of the structures of **1** and **3-13** in DMSO/H_2O solution, derived from spectroscopic studies, with the biological data allowed evaluation of the influence of the substituent structure at C(3) atom on antibacterial properties of this type of derivatives. A comparison of the biological test results against Gram-(+) bacteria strains indicates that the analogues comprising chlorine atom at *m*- and *p*- positions of phenyl ring (compounds **8** and **9**) are the least active of all other amino analogues synthesised. Furthermore, as follows from analysis of the biological data of all **3-13** amino analogues, the ones containing substituents at *m*- and *p*- positions at phenyl ring are slightly less active than those comprising unsubstituted or substituted phenyl ring at *o*-position. Thus, slightly increased biological properties of compounds **3**, **4**, **7**, **10** and **11** are result of the presence of the less bulky substituents at C(3) position, i.e. there is no substituted halogen at phenyl ring or the halogen atom is less distanced from *ipso* position. Taking into account antibacterial properties of **3-13** amino analogues of rifampicin and the fact that the substituent at C(3) due to the presence of a secondary amine linker cannot be easily hydrolized by bacteria (one of the processes evoking bacteria resistance to rifampicin) this group of derivatives can be interesting for further search for rifampicin alternatives. Our studies have shown that not only the structure of *ansa* bridge but also the structure of the substituent at C(3) atom strongly influences the biological properties of this type of *ansa* macrolides.

New model of bacterial RNAP inhibition *via* rifampicin-based *ansa* macrolides

The fact that **1** shows much higher antibacterial properties against standard bacteria strains than **3-13** analogues and that in DMSO/H_2O solution the former is present in the zwitterionic form with the proton localised at the piperazine ring[9] and the latter ones are present in similar conditions as zwitterions with the proton localised at the nitrogen atom of secondary amine, suggests that localisation of proton in the structures of the antibiotics studied plays a crucial role

in inhibition of bacterial RNA polymerase. Taking into account the recently corrected rifampicin pentahydrate structure[10] and the fact that incorrect phenolic form was used for explanation of RNAP inhibition and that the role of the substituent structure at C(3) was neglected[5], it was necessary to propose a new model of inhibition of RNA polymerase *via* zwitterionic forms of **1** and **3-13,** whose presence is unambiguously evidenced by FT-IR and 1D and 2D NMR in solution. Results of molecular docking for **1** and **12** at the binding site of RNAP (which is distanced about 12Å from Mg^{2+} cation and localised at the β subunit deep within DNA/RNA channel) together with the results of optimisation of the interactions between inhibitor and RNAP complex *via* PM5 method are shown in Figures 9 and 10. Intermolecular hydrogen bond parameters calculated for the complexes' structures with RNAP are collected in Table 3. PM5 calculations revealed that the following aminoacids: Q_{393}, S_{411}, F_{394}, R_{409} and D_{396} are involved in stabilisation of both **1** and **12** molecules at RNAP binding site. Difference in bonding of **1** and **12** to RNAP is related to participation of the substituent at C(3) atom in intermolecular hydrogen bond, so instead of the interaction with E_{445} for **1**, that with N_{448} is realised for **12**. As follows from the calculations, the side chains of the following amino acids: I_{452}, Q_{390}, L_{413} and G_{414} participate mainly in hydrophobic stabilisation of the complex between the inhibitors and RNAP, which is in agreement with the model of RNAP inhibition proposed by Darst et al.[5] It has been earlier suggested that also H_{406} is involved in **1** binding to RNAP[5] but our calculations do not support its role in hydrogen-bonding of the inhibitor molecule (parameters collected in Table 3). A comparison of hydrogen bond parameters in Table 3 demonstrates that for **1** and **12** docked as zwitterions, the *ansa* bridge bonding to aminoacids of RNAP is realised in a similar way, i.e. the type and strength of the interactions are comparable. A very important role in stabilisation of the inhibitor molecule in the complex with RNAP is played by F_{394} which acts simultaneously as donor and acceptor of proton in the two hydrogen bonds formed with the oxygen of C(35)=O of acetate and with the proton of O(23)H hydroxyl of the *ansa*-bridge, respectively. Higher electron density at O(8) atom in the zwitterionic forms of **1** and **3-13** favours the enhancement of intermolecular hydrogen bonds with the proton of S_{411} hydroxyl group and with the proton of Q_{393} amide group. Thus, if the *ansa* bridge is bonded in a similar way in **1** and **3-13**, the presence or absence of intermolecularly hydrogen bonded substituent at C(3) is essential. If compared the nature and parameters of the intermolecular hydrogen bonds formed between RNAP polymerase and the protons transferred from O(8)H group in **1** or **12**: for RNAP-**12** complex hydrogen bond

with N_{448} is of medium strength (donor-acceptor distance 2.73 Å, angle 140°, Fig. 9a) whereas the respective one with E_{445} for RNAP-**1** complex is very strong and of acid-amine salt character (donor-acceptor distance 2.57 Å, angle 176°, Fig. 9b), the significant differences in antibacterial properties between **1** and **3-13** are understandable. For recently obtained alkyl analogues containing terminal hydroxyls[9] the flexible aliphatic chains with OH group will be rather directed outside and probably solvated by water molecules than bonded to E_{445} *via* a definitely weaker interaction of different character $_{alkyl}CH_2O\text{-}H^{\cdots}{}^{-}O_{carboxylate}(E_{445})$ than that of salt character postulated for **1** $[_{piperazine}N(40)^{+}\text{-}H^{\cdots}{}^{-}O_{carboxylate}(E_{445})]$. Thus, the rigidity of the moiety at C-3 position which acts as proton donor is also an important factor which influences additionally formation of intermolecular hydrogen bond with E_{445}. For **1** spatial fit and intermolecular bonding with E_{445} of RNAP contributes to exposition of hydrophobic part of the piperazine ring to external environment which additionally protects this structural part of the antibiotic against solvation process. It should be mentioned here that E_{445} at the binding site is unsusceptible to the mutation processes in bacteria which is explained by too far-reached structural changes in RNAP resulting in its complete inactivation.[5,17,18] If a bulky substituent such as a phenyl ring or a substituted with halogen phenyl ring, cannot take part in analogous interaction with E_{445} of salt character (Fig. 10a), it is directed outside and in consequence destabilises rather than stabilizes the inhibitor-RNAP complex (Fig. 10b). As shown by the calculated structures (Figs. 9 and 10) after bonding of **1** or **12** to bacterial RNAP the intramolecular O(8)$^{\cdots}$H-O(1) hydrogen bonds (for **1** and **12**), N(2)-H$^{\cdots}$N=C(38) bond for **1** and $N(38)^{+}$-H$^{\cdots}$O=C(15) bond for **12** are conserved in relation to the respective ones formed for **1** and **12** molecules in solution. The weak π-π stacking interaction between electrons of diene and phenyl ring realised in the structure of **12** in solution, is broken with the formation of **12**-RNAP complex.

Conclusions

Reductive amination of 3-formylrifamycin SV toward efficient synthesis of analogues **3-13** has been optimised. On the basis of FT-IR and ^{1}H, ^{13}C and ^{15}N and 2D NMR studies, in solution the presence of zwitterionic forms of **1** and its **3-13** analogues with the proton transferred from O(8)H phenol group to tertiary and secondary nitrogen atom of amine moieties, respectively, has been evidenced. The zwitterionic forms of **1** and **3-13** are stabilised *via* several intramolecular hydrogen bonds of which the one O(1)-H$^{\cdots}$O(8), formed in a six membered system, is the

strongest. ^{1}H-^{1}H NOESY studies on conformation of the new amino analogues **3-13** revealed two different orientations in solution of the substituent at C(3) atom. In solution in **3-9** benzyl analogues the substituent is distanced away from the *ansa*-bridge whereas in the structure of **10-13** phenethyl analogues the phenyl ring of the substituent at C(3) is involved in π-π interactions with the diene moiety of the *ansa*-bridge. The activity level of analogues **3-13**, comparable to those of other antibiotics as e.g. ciprofloxacin (especially against *S. epidermidis* strains) and the presence of C(38)-N bond resistant to hydrolysis by bacteria, make this type of derivatives promising for further search to enhance the biological properties. Taking into account the presence of zwitterionic forms of **1**, **3-13** and other earlier reported derivatives[9] in protic and aprotic solvents with addition of water and comparison of their biological data with the results of respective molecular recognition studies, it has been revealed that in effective RNAP inhibition the strongest intermolecular hydrogen bond of salt character between protonated amine moiety of the substituent at C(3) and E_{445} plays a very important role. The calculated interactions between the *ansa*-bridge of the antibiotics and the enzyme suggests that this structural fragment is relatively flexible and is bonded similarly both for **1** and for its analogues, irrespectively of the structure substituent at C-3 atom (*o*-, *m*-, *p*- substitution). New model of inhibition of bacterial RNAP proposed here is in agreement with our earlier structural spectroscopic, X-ray and antibacterial studies[9,10] and, in contrast to earlier proposed model, explains the differences in antibacterial properties between **1** and its aliphatic[9] and aromatic amino analogues. Furthermore, our results suggested that optimisation of biological activity of this group of antibiotics should be performed *via* introducing into chain at C-3 position additional secondary or tertiary amines in a relatively rigid moiety, which will facilitate strong interaction of salt character with E_{445}. This issue is currently under investigation by us and will be reported later.

Experimental

General

DMSO-d_6, $CDCl_3$, DMSO, and $CHCl_3$ for spectroscopic measurements as well as benzylamine, 2-chlorobenzylamine, 3-chlorobenzylamine, 4-chlorobenzylamine, 2-fluorobenzylamine, 3-fluorobenzylamine, 4-fluorobenzylamine, phenethylamine, 2-fluorophenethylamine, 3-fluorophenethylamine, 4-fluorophenethylamine used for syntheses of new rifampicin analogues

were purchased from Aldrich. The reductants $NaBH_4$, $NaBH_3CN$, $NaBH(CH_3COO)_3$ and BH_3CN^- on polymer support and $ZnCl_2$ were purchased from Aldrich.

The ^1H, ^{13}C and ^{15}N measurements of **1-13** were performed in $CDCl_3$ and DMSO-d_6 using Varian Mercury 400 MHz and Bruker Avance 600 MHz spectrometers. The operating frequencies for ^1H measurements were 400.075 and 600.08 MHz; pulse width corresponding to the flip angle of 45^0; spectral width, swh = 9842.5 Hz; acquisition time at= 0.2 sec; relaxation delay d_1=1.0 s; T = 293.0 K, TMS was used as the internal standard. No window function or zero filling were used. Digital resolution was 0.2 Hz/point. ^{13}C NMR spectra were recorded at the operating frequency 150.454 MHz; pulse width corresponding to the flip angle of 60^0; sw = 19000 Hz; at = 1.8 s; d_1=1.0 s; T = 293.0 K and TMS as the internal standard. Line broadening parameters of 0.5 or 1 Hz were applied. ^1H, ^{13}C and ^{15}N NMR resonances were unambiguously assigned on the basis of the HMBC, HSQC, COSY and NOESY correlation spectra.

The FT-IR spectra of **1-13** compounds were recorded in KBr pellet (1.5 mg/200 mg) and DMSO (0.05 mol dm^{-3}) whereas the spectrum of 1:1 **1**-KOH mixture was measured in $CHCl_3$. All FT-IR spectra were recorded with an IFS 113v FT-IR spectrophotometer (Bruker, Karlsruhe) equipped with a DTGS detector; resolution 2 cm^{-1}, NSS = 125, range 4000-400 cm^{-1}. The Happ-Genzel apodization function was used.

The HR-MALDI-TOF spectra of **2** and **3-13** analogues were obtained on Water/Micromass (Manchester, UK) Q-TOF Premier mass spectrometer (software MassLynx V4.1, Manchester, UK) fitted with a 200 Hz repetition rate Nd/YAG (λ = 355 nm, power density 107 W/cm^2). The compounds analysed were solids and the matrix used was DHB.

The elemental analysis of new rifampicin analogues **3-13** and **2** was carried out on Vario ELIII (Elementar, Germany).

PM5 calculations of amino analogues of rifampicin structures as well as interactions between **1** or **12** and bacterial RNA polymerase (RNAP) binding site were performed with the use of *Cache WorkSystem Pro version 7.5.0.85* (*WinMopac 2007* program).[19] The initial model of **1** and **12** structures was built on the basis of the previously determined X-ray structures of zwitterions[9] and X-ray structure of polymerase RNA[5] and then optimised *via* PM5 calculations at the semi-empirical level of theory. The docking of initially optimised structures of **1** and **12** compounds

via PM5 method was performed *via* "dock into active site" function of WinMopac 2007 program. Docking of inhibitor molecules **1** and **12** was performed on previously reported coordinates of naphthalene ring of rifampicin, known from X-ray structure of RNAP[5]. The interactions between **1** molecule, docked as zwitterion, and the aminoacid residues at the binding site to RNAP were modelled *via* geometry calculation in MOPAC using PM5 parameters (Cache Work System Pro Version 7.5.085 – Fujitsu), with the energy gradient not exceeding 2 kcal mol^{-1} at one step (3678 steps). The interactions between **12** inhibitor molecule, docked as zwitterion, and the aminoacid residues at the binding site to RNAP were performed *via* geometry calculation in MOPAC using PM5 parameters, with the energy gradient not exceeding 2 kcal mol^{-1} at one step (4122 steps). Peptide chains of RNAP subunits were locked on α carbon atoms and nitrogen atoms of peptide bonds and the other part of RNA polymerase at 30 Å distance from the binding site was locked totally before ligand-enzyme complex calculations. Structures of complexes made by **1** or **12** inhibitors and RNAP were further optimised with the *PM5 MOZYME* geometry algorithm suitable for large molecules. In the new postulated model of RNAP inhibition the orientation and conformation of the key E_{445} aminoacid residue was conserved as in the X-ray structure of RNAP[5].

Procedure for hydrolysis of rifampicin

To rifampicin (1.06 g, 1.25 mmol) dissolved in diethyl ether (1000 ml), a portion of 250 ml of 0.2 M HCl/H_2O was added and the mixture was stirred for four days at room temperature. Then the organic layer was separated, twice washed with 300 ml of water and evaporated. To crude rifaldehyde, 150 ml CH_2Cl_2 was added and the contents were extracted with 100 ml of brine and separated. Organic layer was evaporated to dryness yielding rifaldehyde (**2**) as red powder (830.2 mg; Yield: 88.9%).

Spectral data for **2**: m.p. = 180-185°C; HR-MALDI-TOF $[M+H]^+$ 726.3111; ^1H NMR (δ ppm in $CDCl_3$): 13.75 (1H, s, NH_{amide}), 12.65 (1H, s, HO-4), 12.30 (1H, s, HO-1), 10.65 (1H, s, H-38), 6.57 (1H, dd, $^3J_{H18\text{-}H19}$=14.9 Hz, H-18), 6.51 (1H, d, $^3J_{H17\text{-}H18}$=11.4 Hz, H-17), 6.24 (1H, d, H-29), 6.07 (1H, dd, $^3J_{H19\text{-}H20}$=5.0 Hz, H-19), 4.94 (1H, d, $^3J_{H25\text{-}H26}$=10.0 Hz, H-25), 5.12 (1H, dd, $^3J_{H28\text{-}H29}$=12.7 Hz, H-28), 3.78 (1H, d, $^3J_{H17\text{-}H18}$=9.5 Hz, H-21), 3.63 (1H, bs, HO-23), 3.55 (1H, bs, HO-21), 3.51 (1H, d, $^3J_{H27\text{-}H28}$=7.0 Hz, H-27), 3.05 (3H, s, H-37), 3.05 (1H, m, H-23),

2.43 (1H, m, H-20), 2.27 (3H, s, H-14), 2.07 (3H, s, H-30), 2.06 (3H, s, H-36), 1.82 (3H, s, H-13), 1.76 (1H, m, H-22), 1.54 (1H, qd, $^{3}J_{H24\text{-}H33}$=6.8 Hz, $^{3}J_{H23\text{-}H24}$=14.0 Hz, H-24), 1.37 (1H, m, H-26), 1.03 (3H, d, $^{3}J_{H22\text{-}H32}$=7.0 Hz, H-32), 0.91 (3H, d, $^{3}J_{H20\text{-}H31}$=7.0 Hz, H-31), 0.67 (3H, d, $^{3}J_{H24\text{-}H33}$=6.9 Hz, H-33), -0.30 (3H, d, $^{3}J_{H26\text{-}H34}$=6.9 Hz, H-34); ^{13}C NMR (δ ppm in $CDCl_3$): 196.6 (C-11), 194.1 (C-38), 174.8 (C-8), 172.1 (C-35), 170.4 (C-15), 168.6 (C-6), 156.0 (C-4), 143.7 (C-19), 142.8 (C-29), 137.8 (C-1), 136.9 (C-17), 127.8 (C-16), 122.6 (C-18), 120.6 (C-2), 119.4 (C-28), 119.1 (C-10), 117.4 (C-9), 109.7 (C-3), 109.5 (C-7), 109.2 (C-12), 105.5 (C-5), 77.0 (C-23), 76.5 (C-27), 74.2 (C-25), 70.7 (C-21), 57.1 (C-37), 39.6 (C-26), 38.6 (C-20), 37.6 (C-24), 33.3 (C-22), 21.5 (C-13), 20.7 (C-36), 20.5 (C-30), 16.9 (C-31), 10.9 (C-32), 9.1 (C-34), 8.6 (C-33), 7.8 (C-14); ^{1}H and ^{13}C resonance assignments were confirmed by COSY, HSQC, HMBC and NOESY 2D correlations; FT-IR (KBr, 1.5 mg): 3415 cm^{-1} $\nu(O_{21}\text{-}H)+\nu(O_{23}\text{-}H)$, 3200 cm^{-1} $\nu(O_8\text{-}H\cdots O_1)+\nu(O_4\text{-}H\cdots O_{11})+ \nu(O_1\text{-}H\cdots O_{15})$, 2550 cm^{-1} $\nu(N\text{-}H_{amide})$, 1726 cm^{-1} $\nu(C_{35}=O)$, 1654 cm^{-1} $\nu(C_{38}=O)_{aldehyde}+ \nu(C_{15}=O)_{amide\ I}$, 1642 cm^{-1} $\nu(C_{11}=O)_{ketone}$, 1575 cm^{-1} $\nu(C\text{-}N)_{amide\ II}$, 1538 cm^{-1} $\nu(C=C)_{naphthalene}$, 1464 cm^{-1} $\nu(C=C)$, 1249 cm^{-1} $\nu(C\text{-}O)$; Elemental analysis $C_{38}H_{47}NO_{13}$: calculated C=62.89%, H=6.53%, N=1.93%; found C=62.81%, H=6.49%, N=1.85%.

6.3. Methods of synthesis of new halogen benzyl and pheneethyl amino analogues of rifampicin (**3-13**):

Method 1: Rifaldehyde (**2**) (290.0 mg, 0.4 mmol) was dissolved in 30 ml CH_2Cl_2 and *p*-chlorobezylamine (0.41 mmol) in 5 ml of C_2H_5OH with a catalyst (0.2 mmol $ZnCl_2$ or 0.02 mmol HCl/EtOH) added. The mixtures were stirred at 45°C for half an hour and after that a half of solvent volume was distilled off. To the cooled reaction mixture (room temperature) the reductant $NaBH_4$ (6.8 mg, 0.18 mmol) was added portionwise over 1 min. The reaction mixture was evaporated to dryness, dissolved in 50 ml of ethyl acetate and extracted twice with 50 ml of water and brine. The separated organic layer was evaporated and the respective synthesised analogue of rifampicin (compound **9**) was purified by column chromatography with silica gel (25 cm × 1 cm, silica gel 60, 0.040-0.063 mm/230-400 mesh ASTM, Fluka) and ethyl acetate/methanol as eluent (from 100:0 to 15:1). TLC (15:1 ethyl acetate:methanol as eluent) was developed. Compound **9** was obtained as orange solid.

Method 2: Rifaldehyde (**2**) (290.0 mg, 0.4 mmol) was dissolved in 30 ml CH_2Cl_2 and the *p*-chlorobezylamine (0.41 mmol) in 5 ml of C_2H_5OH with a catalyst (0.2 mmol $ZnCl_2$ or 0.02 mmol

HCl/EtOH) added. The mixtures were stirred at 45°C for half an hour and after that a half of the solvent volume was distilled off. To the cooled reaction mixture (room temperature), the reductant $NaBH(CH_3COO)_3$ (93.3 mg, 0.44 mmol) was added portionwise over 1 min. The reaction mixture was evaporated to dryness, dissolved in 50 ml of ethyl acetate and extracted twice with 50 ml of water and brine. The separated organic layer was evaporated and the respective synthesised analogue of rifampicin (compound **9**) was purified by column chromatography with silica gel (25 cm × 1 cm, silica gel 60, 0.040-0.063 mm/230-400 mesh ASTM, Fluka) and ethyl acetate/methanol as an eluent (from 100:0 to 15:1). TLC (15:1 ethyl acetate:methanol as eluent) was developed. Compound **9** was obtained as orange solid.

Method 3: Rifaldehyde (**2**) (290.0 mg, 0.4 mmol) was dissolved in 30 ml CH_2Cl_2 and the respective benzyl or phenethyl amine (0.41 mmol) in 5 ml of C_2H_5OH with a catalyst (0.2 mmol $ZnCl_2$ or 0.02 mmol HCl/EtOH) added. The mixtures were stirred at 45°C for half an hour and after that a half of the solvent volume was distilled off. To the cooled reaction mixture (room temperature), the reductant $NaBH_3CN$ (25.1 mg, 0.4 mmol) was added portionwise over 1 min. The reaction mixture was evaporated to dryness, dissolved in 50 ml of ethyl acetate and extracted twice with 50 ml of water and brine. The separated organic layer was evaporated and the respective synthesised analogues of rifampicin (compounds **3-13**) were purified by column chromatography with silica gel (25 cm × 1 cm, silica gel 60, 0.040-0.063 mm/230-400 mesh ASTM, Fluka) and ethyl acetate/methanol as eluent (from 100:0 to 15:1). TLC (15:1 ethyl acetate:methanol as an eluent) was developed. Compounds **3-13** were obtained as yellow, orange and red solids.

Method 4: Rifaldehyde (**2**) (290.0 mg, 0.4 mmol) was dissolved in 30 ml CH_2Cl_2 and the *p*-chlorobezylamine (0.41 mmol) in 5 ml of C_2H_5OH with a catalyst (0.2 mmol $ZnCl_2$ or 0.02 mmol HCl/EtOH) added. The mixtures were stirred at 45°C for half an hour and after that a half of the solvent volume was distilled off. To the cooled reaction mixture (room temperature), the reductant BH_3CN^- on polymer support (210.0 mg) was added in one step. The organic layer was evaporated to dryness, dissolved in 50 ml of ethyl acetate and extracted twice with 50 ml of water and brine. The separated organic layer was evaporated and the respective synthesised analogue of rifampicin (compound **9**) was purified by column chromatography with silica gel (25 cm × 1 cm, silica gel 60, 0.040-0.063 mm/230-400 mesh ASTM, Fluka) and ethyl acetate/methanol as eluent

(from 100:0 to 15:1). TLC (15:1 ethyl acetate:methanol as eluent) was developed. Compound **9** was obtained as orange solid.

Spectral data for (**3**): Yield 57% /method 3 with HCl(EtOH)/; m.p. 134-135 °C; ESI-MS (*m/z*): 817 $[M+H]^+$; HR-MALDI-TOF (*m/z*) 817.3917 $[M+H]^+$; ^{1}H NMR (δ ppm in DMSO-d_6): 16.02 (1H, bs, OH-1), 12.83 (1H, s, OH-4), 9.27 (1H, s, NH_{amide}), 8.94 (1H, vbs, $N^+H_{intramolecularly\ hydrogen\ bonded}$), 8.54 (1H, vbs, $N^+H_{hydrogen\ bonded\ with\ the\ solvent}$), 7.49 (2H, m, H-41 + H-45), 7.37 (3H, m, H-42 + H-43 + H-44), 6.38 (1H, dd, $^3J_{H18\text{-}H19}$=15.8 Hz, $^3J_{H17\text{-}H18}$=10.8 Hz, H-18), 6.26 (1H, d, H-17), 6.27 (1H, d, $^3J_{H28\text{-}H29}$=13.0 Hz, H-29), 6.00 (1H, dd, $^3J_{H19\text{-}H20}$=7.4 Hz, H-19), 5.06 (1H, d, $^3J_{H25\text{-}H26}$=11.0 Hz, H-25), 5.03 (1H, d, $^3J_{H21\text{-}OH}$=3.1 Hz, OH-21), 4.90 (1H, dd, H-28), 4.24 (2H, m, H-39), 4.20 (1H, m, H-38a), 3.95 (1H, d, $^3J_{H23\text{-}HO}$=8.2 Hz, OH-23), 3.58 (1H, m, H-38b), 3.56 (1H, m, H-21), 3.23 (1H, d, $^3J_{H27\text{-}H28}$=8.9 Hz, H-27), 2.88 (3H, s, H-37), 2.80 (1H, dd, $^3J_{H22\text{-}H23}$=8.4 Hz, $^3J_{H23\text{-}H24}$=9.4 Hz, H-23), 2.24 (1H, m, H-20), 1.97 (3H, s, H-36), 1.94 (3H, s, H-30), 1.92 (3H, s, H-14), 1.65 (3H, s, H-13), 1.62 (1H, m, H-22), 1.22 (1H, m, H-24), 0.95 (1H, m, H-26), 0.89 (3H, d, $^3J_{H22\text{-}H32}$=7.0 Hz, H-32), 0.78 (3H, d, $^3J_{H20\text{-}H31}$=7.0 Hz, H-31), 0.39 (3H, d, $^3J_{H24\text{-}H33}$=7.0 Hz, H-33), -0.37 (3H, d, $^3J_{H26\text{-}H34}$=7.0 Hz, H-34); ^{13}C NMR (δ ppm in DMSO-d_6): 185.3 (C-11), 184.2 (C-8), 171.8 (C-6), 170.3 (C-15), 169.4 (C-35), 148.7 (C-1), 145.0 (C-4), 143.1 (C-29), 139.2 (C-19), 131.8 (C-17) , 131.4 (C-40), 131.0 (C-16), 129.8 (C-41 + C-45), 129.0 (C-43), 128.7 (C-44), 128.4 (C-42), 126.0 (C-18), 118.0 (C-2), 117.6 (C-28), 116.5 (C-10), 115.1 (C-9), 114.7 (C-3), 108.8 (C-12), 101.3 (C-7), 98.6 (C-5), 76.2 (C-27), 75.7 (C-23), 73.1 (C-25), 72.6 (C-21), 55.6 (C-37), 50.2 (C-39), 42.1 (C-38), 40.2 (C-26), 38.1 (C-24), 37.8 (C-20), 32.6 (C-22), 22.1 (C-13), 20.6 (C-36), 19.9 (C-30), 18.2 (C-31), 11.1 (C-32), 9.0 (C-34), 8.6 (C-33), 7.4 (C-14); ^{15}N NMR (δ ppm in DMSO-d_6): -255 (N-2), -329 (N-38); ^{1}H, ^{13}C and ^{15}N resonance assignments were confirmed by COSY, HSQC, HMBC and NOESY 2D spectra; FT-IR (KBr pellet): 3432 and 3401 cm^{-1} $\nu(O_{21}\text{-}H)$ + $\nu(O_{23}\text{-}H)$, 3344 cm^{-1} $\nu(N\text{-}H)_{amide}$, 3143 cm^{-1} $\nu(O_4\text{-}H\cdots O_{11})$, 2740 cm^{-1} $\nu(N_{38}^{+}\text{-}H\cdots O_{15})$, 2468 cm^{-1} $\nu(O_1\text{-}H\cdots O_8^{-})$, 1724 cm^{-1} $\nu(C_{35}{=}O)$, 1646 cm^{-1} $\nu(C_{15}{=}O)_{amide\ I}$, 1597 cm^{-1} ν $(C{=}C)_{naphthtalene}$, 1562 cm^{-1} δ $(N\text{-}H)_{amide\ II}$, 1543 cm^{-1} $\nu(C{=}C)$, 1457 and 1444 cm^{-1} $\nu(C{=}C)_{diene}$, 1247 and 1239 cm^{-1} $\nu(C\text{-}O)$; Elemental analysis (%): Calcd. for $C_{45}H_{56}N_2O_{12}$: C, 66.16; H, 6.91, N, 3.43; Found: C, 66.22; H, 6.87, N, 3.49.

Spectral data for (**4**): Yield 54% /method 3 with HCl(EtOH)/; m.p. 212-213 °C; ESI-MS (*m/z*): 835 $[M+H]^+$; HR-MALDI-TOF (*m/z*) 835.3818 $[M+H]^+$; ^{1}H NMR (δ ppm in DMSO-d_6): 16.04

(1H, bs, OH-1), 12.85 (1H, s, OH-4), 9.29 (1H, s, NH_{amide}), 9.01 (1H, vbs, $N^{+}H_{intramolecularly\ hydrogen\ bonded}$), 8.53 (1H, vbs, $N^{+}H_{hydrogen\ bonded\ with\ the\ solvent}$), 7.61 (1H, dt, $^{3}J_{H44\text{-}H45}$=8.8 Hz, $^{3}J_{H45\text{-}F}$=5.5 Hz, H-45), 7.46 (1H, tdd, $^{3}J_{H42\text{-}H43}$=7.7 Hz, $^{3}J_{H43\text{-}H44}$=7.7 Hz, $^{3}J_{H43\text{-}F}$=5.6 Hz, $^{4}J_{H43\text{-}H45}$=1.8 Hz, H-43), 7.23 (1H, m, H-44), 7.21 (1H, m, H-42), 6.40 (1H, dd, $^{3}J_{H18\text{-}H19}$=15.9 Hz, $^{3}J_{H17\text{-}H18}$=10.8 Hz, H-18), 6.25 (1H, d, $^{3}J_{H28\text{-}H29}$=12.9 Hz, H-29), 6.22 (1H, d, H-17), 6.03 (1H, dd, $^{3}J_{H19\text{-}H20}$=7.2 Hz, H-19), 5.08 (1H, d, $^{3}J_{H25\text{-}H26}$=11.0 Hz, H-25), 5.03 (1H, d, $^{3}J_{H21\text{-}HO}$=3.1 Hz, OH-21), 4.91 (1H, dd, H-28), 4.30 (2H, m, H-39), 4.27 (1H, m, H-38a), 3.98 (1H, d, $^{3}J_{H23\text{-}HO}$=8.6 Hz, OH-23), 3.65 (1H, m, H-21), 3.61 (1H, m, H-38b), 3.24 (1H, d, $^{3}J_{H27\text{-}H28}$=8.7 Hz, H-27), 2.89 (3H, s, H-37), 2.83 (1H, m, H-23), 2.26 (1H, m, H-20), 1.98 (3H, s, H-36), 1.92 (3H, s, H-30), 1.89 (3H, s, H-14), 1.70 (1H, m, H-22), 1.65 (3H, s, H-13), 1.22 (1H, m, H-24), 0.97 (1H, m, H-26), 0.91 (3H, d, $^{3}J_{H22\text{-}H32}$=7.2 Hz, H-32), 0.86 (3H, d, $^{3}J_{H20\text{-}H31}$=7.0 Hz, H-31), 0.45 (3H, d, $^{3}J_{H24\text{-}H33}$=7.0 Hz, H-33), -0.36 (3H, d, $^{3}J_{H26\text{-}H34}$=6.8 Hz, H-34); ^{13}C NMR (δ ppm in DMSO-d_6): 185.3 (C-11), 184.1 (C-8), 171.8 (C-6), 170.2 (C-15), 169.3 (C-35), 160.8 (d, $^{2}J_{C\text{-}F}$=247.0 Hz, C-41), 148.6 (C-1), 145.0 (C-4), 143.0 (C-29), 139.0 (C-19), 132.1 (bs, C-45), 131.9 (C-17), 131.8 (d, $^{3}J_{C\text{-}F}$=8.4 Hz, C-43), 130.7 (C-16), 125.8 (C-18), 124.8 (bs, C-44), 118.4 (d, $^{2}J_{C\text{-}F}$=14.4 Hz, C-40), 117.9 (C-2), 117.6 (C-28), 116.4 (C-10), 115.5 (d, $^{2}J_{C\text{-}F}$=20.9 Hz, C-42), 115.1 (C-3 + C-9), 108.8 (C-12), 101.3 (C-7), 98.5 (C-5), 76.3 (C-27), 75.7 (C-23), 73.2 (C-25), 72.6 (C-21), 55.6 (C-37), 43.4 (C-39), 42.3 (C-38), 40.2 (C-26), 38.2 (C-24), 37.8 (C-20), 32.6 (C-22), 22.0 (C-13), 20.7 (C-36), 19.8 (C-30), 18.1 (C-31), 11.0 (C-32), 8.9 (C-34), 8.5 (C-33), 7.3 (C-14); ^{15}N NMR (δ ppm in DMSO-d_6): -252 (N-2), -333 (N-38); ^{1}H, ^{13}C and ^{15}N resonance assignments were confirmed by COSY, HSQC, HMBC and NOESY 2D spectra; FT-IR (KBr pellet): 3435 and 3408 cm^{-1} $\nu(O_{21}\text{-}H) + \nu(O_{23}\text{-}H)$, 3352 cm^{-1} $\nu(N\text{-}H)_{amide}$, 3151 cm^{-1} $\nu(O_4\text{-}H\cdots O_{11})$, 2746 cm^{-1} $\nu(N_{38}^{+}\text{-}H\cdots O_{15})$, 2465 cm^{-1} $\nu(O_1\text{-}H\cdots O_8^{-})$, 1721 cm^{-1} $\nu(C_{35}{=}O)$, 1641 cm^{-1} $\nu(C_{15}{=}O)_{amide\ I}$, 1601 cm^{-1} $\nu(C{=}C)_{naphthalene}$, 1567 cm^{-1} $\delta(N\text{-}H)_{amide\ II}$, 1541 cm^{-1} $\nu(C{=}C)_{diene}$, 1459 and 1443 cm^{-1} $\nu(C{=}C)$, 1243 and 1231 cm^{-1} $\nu(C\text{-}O)$; Elemental analysis (%): Calcd. for $C_{45}H_{55}FN_2O_{12}$: C, 64.73; H, 6.64, N, 3.36; Found: C, 64.80; H, 6.58, N, 3.32.

Spectral data for (**5**): Yield 59% /method 3 with HCl(EtOH)/; m.p. 189-190 °C; ESI-MS (*m/z*): 835 $[M+H]^{+}$; HR-MALDI-TOF (*m/z*) 835.3805 $[M+H]^{+}$; ^{1}H NMR (δ ppm in DMSO-d_6): 16.02 (1H, bs, OH-1), 12.85 (1H, s, OH-4), 9.26 (1H, s, NH_{amide}), 9.03 (1H, vbs, $N^{+}H_{intramolecularly\ hydrogen\ bonded}$), 8.52 (1H, vbs, $N^{+}H_{hydrogen\ bonded\ with\ the\ solvent}$), 7.39 (1H, m, H-44), 7.37 (1H, m, H-45), 7.33 (1H, m, H-41), 7.20 (1H, m, H-43), 6.32 (1H, dd, $^{3}J_{H18\text{-}H19}$=15.6 Hz, $^{3}J_{H17\text{-}H18}$=11.0 Hz, H-18),

6.24 (1H, d, H-17), 6.26 (1H, d, $^{3}J_{H28\text{-}H29}$=13.0 Hz, H-29), 6.00 (1H, dd, $^{3}J_{H19\text{-}H20}$=7.4 Hz, H-19), 5.06 (1H, d, $^{3}J_{H25\text{-}H26}$=11.0 Hz, H-25), 5.03 (1H, d, $^{3}J_{H21\text{-}HO}$=3.1 Hz, OH-21), 4.90 (1H, dd, H-28), 4.26 (2H, m, H-39), 4.20 (1H, m, H-38a), 3.92 (1H, d, $^{3}J_{H23\text{-}HO}$=8.2 Hz, OH-23), 3.56 (1H, m, H-21), 3.51 (1H, m, H-38b), 3.23 (1H, d, $^{3}J_{H27\text{-}H28}$=8.9 Hz, H-27), 2.88 (3H, s, H-37), 2.80 (1H, dd, $^{3}J_{H22\text{-}H23}$=8.4 Hz, $^{3}J_{H23\text{-}H24}$=9.4 Hz, H-23), 2.22 (1H, m, H-20), 1.98 (3H, s, H-36), 1.93 (3H, s, H-30), 1.91 (3H, s, H-14), 1.65 (3H, s, H-13), 1.61 (1H, m, H-22), 1.21 (1H, m, H-24), 0.96 (1H, m, H-26), 0.89 (3H, d, $^{3}J_{H22\text{-}H32}$=7.0 Hz, H-32), 0.75 (3H, d, $^{3}J_{H20\text{-}H31}$=6.8 Hz, H-31), 0.41 (3H, d, $^{3}J_{H24\text{-}H33}$=6.7 Hz, H-33), -0.38 (3H, d, $^{3}J_{H26\text{-}H34}$=6.7 Hz, H-34); ^{13}C NMR (δ ppm in DMSO-d_6): 185.3 (C-11), 184.2 (C-8), 171.8 (C-6), 170.2 (C-15), 169.4 (C-35), 162.0 (d, $^{1}J_{C\text{-}F}$=244.8 Hz, C-42), 148.7 (C-1), 145.1 (C-4), 143.2 (C-29), 139.0 (C-19), 133.9 (d, $^{3}J_{C\text{-}F}$=8.0 Hz, C-40), 131.9 (C-17), 130.9 (C-16), 130.8 (d, $^{3}J_{C\text{-}F}$=8.2 Hz, C-44), 126.1 (d, $^{4}J_{C\text{-}F}$=2.9 Hz, C-45), 125.9 (C-18), 118.0 (C-2), 117.6 (C-28), 116.8 (d, $^{2}J_{C\text{-}F}$=21.9 Hz, C-41), 116.5 (C-10), 115.9 (d, $^{2}J_{C\text{-}F}$=19.8 Hz, C-43), 115.2 (C-9), 114.8 (C-3), 108.9 (C-12), 101.4 (C-7), 98.6 (C-5), 76.3 (C-27), 75.7 (C-23), 73.2 (C-25), 72.7 (C-21), 55.7 (C-37), 49.6 (C-39), 42.0 (C-38), 40.3 (C-26), 38.2 (C-24), 37.7 (C-20), 32.6 (C-22), 22.1 (C-13), 20.7 (C-36), 19.9 (C-30), 18.2 (C-31), 11.0 (C-32), 9.1 (C-34), 8.7 (C-33), 7.4 (C-14); ^{15}N NMR (δ ppm in DMSO-d_6): -252 (N-2), -334 (N-38); ^{1}H, ^{13}C and ^{15}N resonance assignments were confirmed by COSY, HSQC, HMBC and NOESY 2D spectra; FT-IR (KBr pellet): 3439 and 3413 cm^{-1} ν(O_{21}-H) + ν(O_{23}-H), 3339 cm^{-1} ν(N-H)$_{amide}$, 3154 cm^{-1} ν(O_4-H···O_{11}), 2751 cm^{-1} ν(N_{38}+-H···O_{15}), 2461 cm^{-1} ν(O_1-H···O_8^-), 1719 cm^{-1} ν(C_{35}=O), 1639 cm^{-1} ν(C_{15}=O)$_{amide\ I}$, 1598 cm^{-1} ν(C=C)$_{naphthalene}$,1561 cm^{-1} δ(N-H)$_{amide\ II}$, 1539 cm^{-1} ν(C=C), 1451 and 1438 cm^{-1} ν(C=C), 1249 and 1232 cm^{-1} ν(C-O); Elemental analysis (%): Calcd. for $C_{45}H_{55}FN_2O_{12}$: C, 64.73; H, 6.64, N, 3.36; Found: C, 64.66; H, 6.69, N, 3.44.

Spectral data for (**6**): Yield 56% /method 3 with HCl(EtOH)/; 169-171 °C; ESI-MS (*m/z*): 835 $[M+H]^+$; HR-MALDI-TOF (*m/z*) 835.3821 $[M+H]^+$; ^{1}H NMR (δ ppm in DMSO-d_6): 16.03 (1H, bs, OH-1), 12.84 (1H, s, OH-4), 9.26 (1H, s, NH_{amide}), 8.95 (1H, vbs, $N^+H_{intramolecularly\ hydrogen\ bonded}$), 8.45 (1H, vbs, $N^+H_{hydrogen\ bonded\ with\ the\ solvent}$), 7.55 (2H, dd, $^{3}J_{H41\text{-}H42/H44\text{-}H45}$=8.8 Hz, $^{3}J_{H41\text{-}F/H45\text{-}F}$=5.5 Hz, H-41 + H-45), 7.39 (2H, t, $^{2}J_{H42\text{-}F/H44\text{-}F}$=8.6 Hz, H-42 + H-44), 6.32 (1H, dd, $^{3}J_{H18\text{-}H19}$=15.2 Hz, $^{3}J_{H17\text{-}H18}$=10.7 Hz, H-18), 6.26 (1H, d, $^{3}J_{H28\text{-}H29}$=12.8 Hz, H-29), 6.25 (1H, d, H-17), 6.02 (1H, dd, $^{3}J_{H19\text{-}H20}$=7.5 Hz, H-19), 5.07 (1H, d, $^{3}J_{H25\text{-}H26}$=11.0 Hz, H-25), 5.03 (1H, d, $^{3}J_{H21\text{-}HO}$=3.1 Hz, OH-21), 4.90 (1H, dd, H-28), 4.24 (2H, m, H-39), 4.19 (1H, d, =12.0 Hz, H-38a), 3.99 (1H, d, $^{3}J_{H23\text{-}HO}$=8.7 Hz, OH-23), 3.57 (1H, m, H-21), 3.50 (1H, d, H-38b), 3.24 (1H, d,

$^{3}J_{H27\text{-}H28}$=8.9 Hz, H-27), 2.88 (3H, s, H-37), 2.81 (1H, m, H-23), 2.24 (1H, m, H-20), 1.98 (3H, s, H-36), 1.92 (6H, s, H-14 + H-30), 1.65 (3H, s, H-13), 1.62 (1H, m, H-22), 1.22 (1H, m, H-24), 0.96 (1H, m, H-26), 0.90 (3H, d, $^{3}J_{H22\text{-}H32}$=7.0 Hz, H-32), 0.78 (3H, d, $^{3}J_{H20\text{-}H31}$=7.0 Hz, H-31), 0.43 (3H, d, $^{3}J_{H24\text{-}H33}$=6.7 Hz, H-33), -0.37 (3H, d, $^{3}J_{H26\text{-}H34}$=6.7 Hz, H-34); ^{13}C NMR (δ ppm in DMSO-d_6): 185.5 (C-11), 184.2 (C-8), 171.9 (C-6), 170.4 (C-15), 169.4 (C-35), 162.4 (d, $^{1}J_{C\text{-}F}$=245.4 Hz, C-43), 148.7 (C-1), 145.1 (C-4), 143.1 (C-29), 139.0 (C-19), 132.3 (d, $^{3}J_{C\text{-}F}$=8.2 Hz, C-41 + C-45), 131.9 (C-17), 130.9 (C-16), 127.6 (d, $^{4}J_{C\text{-}F}$=2.2 Hz, C-40), 125.9 (C-18), 118.0 (C-2), 117.6 (C-28), 116.5 (C-10), 115.6 (d, $^{2}J_{C\text{-}F}$=21.7 Hz, C-42 + C-44), 115.2 (C-9), 114.8 (C-3), 108.8 (C-12), 101.5 (C-7), 98.6 (C-5), 76.3 (C-27), 75.7 (C-23), 73.2 (C-25), 72.7 (C-21), 55.6 (C-37), 49.4 (C-39), 41.8 (C-38), 40.2 (C-26), 38.2 (C-24), 37.7 (C-20), 32.6 (C-22), 22.1 (C-13), 20.7 (C-36), 19.9 (C-30), 18.1 (C-31), 11.0 (C-32), 9.0 (C-34), 8.6 (C-33), 7.4 (C-14); ^{15}N NMR (δ ppm in DMSO-d_6): -253 (N-2), -332 (N-38); ^{1}H, ^{13}C and ^{15}N resonance assignments were confirmed by COSY, HSQC, HMBC and NOESY 2D spectra; FT-IR (KBr pellet): 3429 and 3410 cm^{-1} $\nu(O_{21}\text{-}H) + \nu(O_{23}\text{-}H)$, 3337 cm^{-1} $\nu(N\text{-}H)_{amide}$, 3148 cm^{-1} $\nu(O_4\text{-}H\cdots O_{11})$, 2744 cm^{-1} $\nu(N_{38}^{+}\text{-}H\cdots O_{15})$, 2457 cm^{-1} $\nu(O_1\text{-}H\cdots O_8^{-})$, 1720 cm^{-1} $\nu(C_{35}{=}O)$, 1644 cm^{-1} $\nu(C_{15}{=}O)_{amide\ I}$, 1596 cm^{-1} $\nu(C{=}C)_{naphthalene}$, 1559 cm^{-1} $\delta(N\text{-}H)_{amide\ II}$, 1542 cm^{-1} $\nu(C{=}C)$, 1449 and 1435 cm^{-1} $\nu(C{=}C)$, 1251 and 1236 cm^{-1} $\nu(C\text{-}O)$; Elemental analysis (%): Calcd. for $C_{45}H_{55}FN_2O_{15}$: C, 64.73; H, 6.64, N, 3.36; Found: C, 64.80; H, 6.61, N, 3.41.

Spectral data for (**7**): Yield 51% /method 3 with HCl(EtOH)/; 165-167 °C; ESI-MS (*m/z*): 835 $[M+H]^{+}$; HR-MALDI-TOF (*m/z*) 851.3522 $[M+H]^{+}$; ^{1}H NMR (δ ppm in DMSO-d_6): 16.02 (1H, bs, OH-1), 12.86 (1H, s, OH-4), 9.30 (1H, s, NH_{amide}), 9.00 (1H, vbs, $N^{+}H_{intramolecularly\ hydrogen\ bonded}$), 8.68 (1H, vbs, $N^{+}H_{hydrogen\ bonded\ with\ the\ solvent}$), 7.68 (1H, dd, $^{3}J_{H42\text{-}H43}$=7.1 Hz, H-42), 7.49 (1H, dd, $^{3}J_{H44\text{-}H45}$=7.5 Hz, $^{4}J_{H43\text{-}H45}$=1.9 Hz,H-45), 7.42 (1H, td, $^{3}J_{H43\text{-}H44}$=7.5 Hz H-43), 7.37 (1H, td, H-44), 6.38 (1H, dd, $^{3}J_{H18\text{-}H19}$=16.1 Hz, $^{3}J_{H17\text{-}H18}$=10.8 Hz, H-18), 6.25 (1H, d, $^{3}J_{H28\text{-}H29}$=12.9 Hz, H-29), 6.21 (1H, d, H-17), 6.02 (1H, dd, $^{3}J_{H19\text{-}H20}$=7.4 Hz, H-19), 5.08 (1H, d, $^{3}J_{H25\text{-}H26}$=10.8 Hz, H-25), 5.03 (1H, d, $^{3}J_{H21\text{-}HO}$=3.1 Hz, OH-21), 4.91 (1H, dd, H-28), 4.38 (2H, m, H-39), 4.30 (1H, d, =11.9 Hz, H-38a), 4.00 (1H, d, $^{3}J_{H23\text{-}HO}$=8.7 Hz, OH-23), 3.65 (1H, m, H-21), 3.61 (1H, m, H-38b), 3.24 (1H, d, $^{3}J_{H27\text{-}H28}$=8.7 Hz, H-27), 2.89 (3H, s, H-37), 2.82 (1H, dd, $^{3}J_{H22\text{-}H23}$=8.4 Hz, $^{3}J_{H23\text{-}H24}$=9.4 Hz, H-23), 2.25 (1H, m, H-20), 1.98 (3H, s, H-36), 1.92 (3H, s, H-30), 1.91 (3H, s, H-14), 1.65 (3H, s, H-13), 1.62 (1H, m, H-22), 1.22 (1H, m, H-24), 0.98 (1H, m, H-26), 0.91 (3H, d, $^{3}J_{H22\text{-}H32}$=7.0 Hz, H-32), 0.85 (3H, d, $^{3}J_{H20\text{-}H31}$=7.0 Hz, H-31), 0.46 (3H, d,

$^{3}J_{H24\text{-}H33}$=7.0 Hz, H-33), -0.37 (3H, d, $^{3}J_{H26\text{-}H34}$=6.8 Hz, H-34); ^{13}C NMR (δ ppm in DMSO-d_6): 185.5 (C-11), 184.2 (C-8), 171.9 (C-6), 170.3 (C-15), 169.5 (C-35), 148.7 (C-1), 145.1 (C-4), 143.1 (C-29), 139.1 (C-19), 134.1 (C-40), 132.3 (C-41), 132.1 (C-17), 131.2 (C-16), 130.6 (C-45), 129.7 (C-42), 129.3 (C-43), 127.8 (C-44), 125.8 (C-18), 118.0 (C-2), 117.6 (C-28), 116.5 (C-10), 115.2 (C-9), 114.6 (C-3), 108.9 (C-12), 101.5 (C-7), 98.6 (C-5), 76.3 (C-27), 75.8 (C-23), 73.2 (C-25), 72.6 (C-21), 55.7 (C-37), 47.4 (C-39), 42.4 (C-38), 40.2 (C-26), 38.2 (C-24), 37.9 (C-20), 32.6 (C-22), 22.1 (C-13), 20.7 (C-36), 19.9 (C-30), 18.3 (C-31), 11.0 (C-32), 9.0 (C-34), 8.7 (C-33), 7.4 (C-14); ^{15}N NMR (δ ppm in DMSO-d_6): -254 (N-2), -334 (N-38); ^{1}H, ^{13}C and ^{15}N resonance assignments were confirmed by COSY, HSQC, HMBC and NOESY 2D spectra; FT-IR (KBr pellet): 3432 and 3414 cm^{-1} $\nu(O_{21}\text{-}H)$ + $\nu(O_{23}\text{-}H)$, 3346 cm^{-1} $\nu(N\text{-}H)_{amide}$, 3153 cm^{-1} $\nu(O_4\text{-}H\cdots O_{11})$, 2741 cm^{-1} $\nu(N_{38}^{+}\text{-}H\cdots O_{15})$, 2452 cm^{-1} $\nu(O_1\text{-}H\cdots O_8^{-})$, 1724 cm^{-1} $\nu(C_{35}{=}O)$, 1649 cm^{-1} $\nu(C_{15}{=}O)_{amide\ I}$, 1599 cm^{-1} $\nu(C{=}C)_{naphthalene}$, 1563 cm^{-1} $\delta(N\text{-}H)_{amide\ II}$, 1544 cm^{-1} $\nu(C{=}C)$, 1446 and 1432 cm^{-1} $\nu(C{=}C)$, 1241 and 1232 cm^{-1} $\nu(C\text{-}O)$; Elemental analysis (%): Calcd. for $C_{45}H_{55}ClN_2O_{15}$: C, 63.48; H, 6.51, N, 3.29; Found: C, 63.53; H, 6.46, N, 3.22.

Spectral data for (**8**): Yield 58% /method 3 with HCl(EtOH)/; m.p. 152-154 °C; ESI-MS (*m/z*): 851 $[M+H]^{+}$; HR-MALDI-TOF (*m/z*) 851.3510 $[M+H]^{+}$; ^{1}H NMR (δ ppm in DMSO-d_6): 16.03 (1H, bs, OH-1), 12.85 (1H, s, OH-4), 9.25 (1H, s, NH_{amide}), 9.02 (1H, vbs, $N^{+}H_{intramolecularly\ hydrogen\ bonded}$), 8.56 (1H, vbs, $N^{+}H_{hydrogen\ bonded\ with\ the\ solvent}$), 7.62 (1H, bs, H-41), 7.47 (1H, m, H-43), 7.39 (1H, m, H-44), 7.43 (1H, m, H-45), 6.33 (1H, dd, $^{3}J_{H18\text{-}H19}$=15.7 Hz, H-18), 6.26 (1H, d, $^{3}J_{H17\text{-}H18}$=10.6 Hz, H-17), 6.23 (1H, d, $^{3}J_{H28\text{-}H29}$=12.9 Hz, H-29), 6.02 (1H, dd, $^{3}J_{H19\text{-}H20}$=7.6 Hz, H-19), 5.06 (1H, d, $^{3}J_{H25\text{-}H26}$=10.5 Hz, H-25), 5.03 (1H, d, $^{3}J_{H21\text{-}HO}$=3.1 Hz, OH-21), 4.91 (1H, dd, H-28), 4.26 (2H, m, H-39), 4.22 (1H, m, H-38a), 3.97 (1H, d, $^{3}J_{H23\text{-}HO}$=6.2 Hz, OH-23), 3.56 (1H, m, H-21), 3.54 (1H, m, H-38b), 3.24 (1H, d, $^{3}J_{H27\text{-}H28}$=8.5 Hz, H-27), 2.88 (3H, s, H-37), 2.81 (1H, dd, $^{3}J_{H22\text{-}H23}$=8.2 Hz, $^{3}J_{H23\text{-}H24}$=8.6 Hz, H-23), 2.27 (1H, m, H-20), 1.98 (3H, s, H-36), 1.95 (3H, s, H-30), 1.91 (3H, s, H-14), 1.65 (3H, s, H-13), 1.62 (1H, m, H-22), 1.19 (1H, m, H-24), 0.97 (1H, m, H-26), 0.90 (3H, d, $^{3}J_{H22\text{-}H32}$=7.0 Hz, H-32), 0.77 (3H, d, $^{3}J_{H20\text{-}H31}$=7.0 Hz, H-31), 0.43 (3H, d, $^{3}J_{H24\text{-}H33}$=7.0 Hz, H-33), -0.36 (3H, d, $^{3}J_{H26\text{-}H34}$=6.8 Hz, H-34); ^{13}C NMR (δ ppm in DMSO-d_6): 185.3 (C-11), 184.1 (C-8), 171.8 (C-6), 170.2 (C-15), 169.3 (C-35), 148.7 (C-1), 145.0 (C-4), 143.1 (C-29), 138.9 (C-19), 133.7 (C-40), 133.3 (C-42), 131.8 (C-17), 130.9 (C-16), 130.5 (C-44), 129.9 (C-41), 129.0 (C-45), 128.7 (C-43), 125.9 (C-18), 118.0 (C-2), 117.7 (C-28), 116.4 (C-10), 115.1 (C-9), 114.6 (C-3), 108.8 (C-12), 101.3 (C-7), 98.5 (C-5), 76.3 (C-27), 75.7 (C-23),

73.2 (C-25), 72.8 (C-21), 55.6 (C-37), 49.5 (C-39), 42.1 (C-38), 40.2 (C-26), 38.1 (C-24), 37.7 (C-20), 32.6 (C-22), 22.0 (C-13), 20.6 (C-36), 19.8 (C-30), 18.2 (C-31), 11.0 (C-32), 9.0 (C-34), 8.6 (C-33), 7.3 (C-14); ^{15}N NMR (δ ppm in DMSO-d_6): -251 (N-2), -330 (N-38); ^{1}H, ^{13}C and ^{15}N resonance assignments were confirmed by COSY, HSQC, HMBC and NOESY 2D spectra; FT-IR (KBr pellet): 3437 and 3396 cm^{-1} ν(O_{21}-H) + ν(O_{23}-H), 3338 cm^{-1} ν(N-H)$_{amide}$, 3150 cm^{-1} ν(O_4-H···O_{11}), 2733 cm^{-1} ν(N_{38}+-H···O_{15}), 2460 cm^{-1} ν(O_1-H···O_8^-), 1721 cm^{-1} ν(C_{35}=O), 1641 cm^{-1} ν(C_{15}=O)$_{amide\ I}$, 1600 cm^{-1} ν(C=C)$_{naphthalene}$, 1558 cm^{-1} δ(N-H)$_{amide\ II}$, 1543 cm^{-1} ν(C=C), 1452 and 1440 cm^{-1} ν(C=C), 1241 and 1229 cm^{-1} ν(C-O); Elemental analysis (%): Calcd. for $C_{45}H_{55}ClN_2O_{12}$: C, 63.48; H, 6.51, N, 3.29; Found: C, 63.41; H, 6.47, N, 3.26.

Spectral data for (**9**): Yield 50% /method 3 with HCl(EtOH)/; m.p. 148-150 °C; ESI-MS (*m/z*): 851 $[M+H]^+$; HR-MALDI-TOF (*m/z*) 851.3514 $[M+H]^+$; ^{1}H NMR (*δ* ppm in DMSO-d_6): 16.01 (1H, bs, OH-1), 12.84 (1H, s, OH-4), 9.24 (1H, s, NH_{amide}), 9.00 (1H, vbs, $N^+H_{intramolecularly\ hydrogen\ bonded}$), 8.43 (1H, vbs, $N^+H_{hydrogen\ bonded\ with\ the\ solvent}$), 7.40 (2H, d, $^3J_{H41\text{-}H42/H44\text{-}H45}$=8.3 Hz, H-41 + H-45), 7.40 (2H, d, H-44), 6.30 (1H, dd, $^3J_{H18\text{-}H19}$=14.9 Hz, $^3J_{H17\text{-}H18}$=10.8 Hz, H-18), 6.26 (1H, d, $^3J_{H28\text{-}H29}$=12.9 Hz, H-29), 6.24 (1H, d, H-17), 6.01 (1H, dd, $^3J_{H19\text{-}H20}$=7.1 Hz, H-19), 5.06 (1H, d, $^3J_{H25\text{-}H26}$=10.2 Hz, H-25), 5.03 (1H, d, $^3J_{H21\text{-}HO}$=3.1 Hz, OH-21), 4.90 (1H, dd, H-28), 4.24 (2H, m, H-39), 4.19 (1H, d, ^2J=12.1 Hz, H-38a), 3.95 (1H, d, $^3J_{H23\text{-}HO}$=8.2 Hz, OH-23), 3.57 (1H, m, H-38b), 3.56 (1H, m, H-21), 3.24 (1H, d, $^3J_{H27\text{-}H28}$=8.8 Hz, H-27), 2.88 (3H, s, H-37), 2.81 (1H, dd, $^3J_{H22\text{-}H23}$=8.9 Hz, $^3J_{H23\text{-}H24}$=9.5 Hz, H-23), 2.24 (1H, m, H-20), 1.98 (3H, s, H-36), 1.92 (3H, s, H-30), 1.91 (3H, s, H-14), 1.65 (3H, s, H-13), 1.62 (1H, m, H-22), 1.18 (1H, m, H-24), 0.97 (1H, m, H-26), 0.90 (3H, d, $^3J_{H22\text{-}H32}$=7.1 Hz, H-32), 0.78 (3H, d, $^3J_{H20\text{-}H31}$=7.1 Hz, H-31), 0.43 (3H, d, $^3J_{H24\text{-}H33}$=6.8 Hz, H-33), -0.38 (3H, d, $^3J_{H26\text{-}H34}$=6.8 Hz, H-34); ^{13}C NMR (*δ* ppm in DMSO-d_6): 185.4 (C-11), 184.2 (C-8), 171.8 (C-6), 170.1 (C-15), 169.4 (C-35), 148.7 (C-1), 145.1 (C-4), 143.2 (C-29), 139.0 (C-19), 132.0 (C-40), 131.9 (C-17), 130.8 (C-16), 130.3 (C-41 + C-45), 128.7 (C-42 + C-44), 125.9 (C-18), 123.9 (C-43), 118.0 (C-2), 117.6 (C-28), 116.5 (C-10), 115.1 (C-9), 114.8 (C-3), 108.9 (C-12), 101.4 (C-7), 98.6 (C-5), 76.3 (C-27), 75.7 (C-23), 73.2 (C-25), 72.6 (C-21), 55.7 (C-37), 49.4 (C-39), 41.8 (C-38), 40.3 (C-26), 38.2 (C-24), 37.7 (C-20), 32.6 (C-22), 22.1 (C-13), 20.7 (C-36), 19.9 (C-30), 18.1 (C-31), 11.0 (C-32), 9.1 (C-34), 8.7 (C-33), 7.4 (C-14); ^{15}N NMR (δ ppm in DMSO-d_6): -253 (N-2), -331 (N-38); ^{1}H, ^{13}C and ^{15}N resonance assignments were confirmed by COSY, HSQC, HMBC and NOESY 2D spectra; FT-IR (KBr pellet): 3437 and 3396 cm^{-1} ν(O_{21}-H) + ν(O_{23}-H), 3338 cm^{-1} ν(N-H)$_{amide}$, 3150 cm^{-1} ν(O_4-

H···O_{11}), 2733 cm^{-1} ν(N_{38}+-H···O_{15}), 2460 cm^{-1} ν(O_1-H···O_8^-), 1721 cm^{-1} ν(C_{35}=O), 1641 cm^{-1} ν(C_{15}=O)$_{amide\ I}$, 1600 cm^{-1} ν(C=C)$_{naphahlene}$, 1558 cm^{-1} δ(N-H)$_{amide\ II}$, 1543 cm^{-1} ν(C=C), 1452 and 1440 cm^{-1} ν(C=C), 1241 and 1229 cm^{-1} ν(C-O); Elemental analysis (%): Calcd. for $C_{45}H_{55}ClN_2O_{15}$: C, 63.48; H, 6.51, N, 3.29; Found: C, 63.57; H, 6.44, N, 3.21.

Spectral data for (**10**): Yield 59% /method 3 with HCl(EtOH)/; m.p. 134-136 °C; ESI-MS (*m/z*): 831 $[M+H]^+$; HR-MALDI-TOF (*m/z*) 851.4067 $[M+H]^+$; ^{1}H NMR (*δ* ppm in DMSO-d_6): 16.05 (1H, bs, OH-1), 12.83 (1H, s, OH-4), 9.31 (1H, s, NH_{amide}), 8.59 (1H, vbs, $N^+H_{intramolecularly\ hydrogen\ bonded}$), 8.36 (1H, vbs, $N^+H_{hydrogen\ bonded\ with\ the\ solvent}$), 7.32 (2H, m, H-43 + H-45), 7.24 (3H, m, H-42 + H-44 + H-46), 6.61 (1H, dd, $^3J_{H18\text{-}H19}$=15.9 Hz, $^3J_{H17\text{-}H18}$=10.8 Hz, H-18), 6.34 (1H, d, H-17), 6.25 (1H, d, $^3J_{H28\text{-}H29}$=12.9 Hz, H-29), 6.09 (1H, dd, $^3J_{H19\text{-}H20}$=7.9 Hz, H-19), 5.08 (1H, d, $^3J_{H25\text{-}H26}$=11.1 Hz, H-25), 5.03 (1H, d, $^3J_{H21\text{-}HO}$=3.1 Hz, OH-21), 4.91 (1H, dd, H-28), 4.35 (1H, d, ^2J=12.4 Hz, H-38a), 3.94 (1H, d, $^3J_{H23\text{-}HO}$=7.6 Hz, OH-23), 3.69 (1H, m, H-21), 3.73 (1H, d, H-38b), 3.22 (1H, d, $^3J_{H27\text{-}H28}$=9.1 Hz, H-27), 3.18 (1H, m, H-39a), 2.94 (2H, m, H-40), 2.89 (3H, s, H-37), 2.83 (1H, dd, $^3J_{H22\text{-}H23}$=8.8 Hz, $^3J_{H23\text{-}H24}$=9.0 Hz, H-23), 2.28 (1H, m, H-20), 1.98 (3H, s, H-36), 1.97 (3H, s, H-30), 1.91 (3H, s, H-14), 1.68 (1H, m, H-22), 1.65 (3H, s, H-13), 1.26 (1H, m, H-24), 0.96 (1H, m, H-26), 0.91 (3H, d, $^3J_{H22\text{-}H32}$=7.1 Hz, H-32), 0.86 (3H, d, $^3J_{H20\text{-}H31}$=7.1 Hz, H-31), 0.51 (3H, d, $^3J_{H24\text{-}H33}$=6.8 Hz, H-33), -0.33 (3H, d, $^3J_{H26\text{-}H34}$=6.8 Hz, H-34); ^{13}C NMR (*δ* ppm in DMSO-d_6): 185.3 (C-11), 184.2 (C-8), 171.8 (C-6), 170.2 (C-15), 169.4 (C-35), 148.9 (C-1), 145.0 (C-4), 143.1 (C-29), 139.1 (C-19), 137.0 (C-41), 131.6 (C-17), 131.4 (C-16), 128.7 (C-43 + C-45), 128.6 (C-42 + C-46), 126.8 (C-44), 126.2 (C-18), 118.0 (C-2), 117.7 (C-28), 116.7 (C-10), 115.1 (C-9), 114.8 (C-3), 108.8 (C-12), 101.3 (C-7), 98.6 (C-5), 76.3 (C-27), 75.8 (C-23), 73.2 (C-25), 72.8 (C-21), 55.6 (C-37), 48.1 (C-39), 43.0 (C-38), 40.3 (C-26), 38.1 (C-24), 37.9 (C-20), 32.7 (C-22), 31.7 (C-40), 22.1 (C-13), 20.7 (C-36), 19.9 (C-30), 18.2 (C-31), 11.2 (C-32), 9.0 (C-34), 8.8 (C-33), 7.4 (C-14); ^{15}N NMR (δ ppm in DMSO-d_6): -254 (N-2), -332 (N-38); ^{1}H, ^{13}C and ^{15}N resonance assignments were confirmed by COSY, HSQC, HMBC and NOESY 2D spectra; FT-IR (KBr pellet): 3448 and 3401 cm^{-1} ν(O_{21}-H) + ν(O_{23}-H), 3345 cm^{-1} ν(N-H)$_{amide}$, 3147 cm^{-1} ν(O_4-H···O_{11}), 2733 cm^{-1} ν(N_{38}^+-H···O_{15}), 2458 cm^{-1} ν(O_1-H···O_8^-), 1721 cm^{-1} ν(C_{35}=O), 1642 cm^{-1} ν(C15=O)$_{amide\ I}$, 1599 cm^{-1} ν(C=C)$_{naphthalene}$, 1553 cm^{-1} δ(N-H)$_{amide\ II}$, 1536 cm^{-1} ν(C=C), 1454 and 1438 cm^{-1} ν(C=C), 1241 and 1228 cm^{-1} ν(C-O); Elemental analysis (%): Calcd. for $C_{45}H_{58}N_2O_{15}$: C, 66.49; H, 7.04, N, 3.37; Found: C, 66.55; H, 6.93, N, 3.40.

Spectral data for (**11**): Yield 57% /method 3 with HCl(EtOH)/; m.p. 150-151°C; ESI-MS (*m/z*): 849 $[M+H]^+$; HR-MALDI-TOF 849.3963 $[M+H]^+$;^{1}H NMR (δ ppm in DMSO-d_6): 16.03 (1H, bs, OH-1), 12.82 (1H, s, OH-4), 9.29 (1H, s, NH_{amide}), 8.65 (1H, bs, $N^+H_{intramolecularly\ hydrogen\ bonded}$), 8.37 (1H, bs, $N^+H_{hydrogen\ bonded\ with\ the\ solvent}$), 7.30 (1H, m, H-44), 7.19 (1H, m, H-45), 7.15 (1H, m, H-43), 7.34 (1H, m, H-46), 6.61 (1H, dd, $^3J_{H18\text{-}H19}$=16.0 Hz, H-18), 6.33 (1H, d, $^3J_{H17\text{-}H18}$=10.6 Hz, H-17), 6.25 (1H, d, , $^3J_{H28\text{-}H29}$=12.9 Hz, H-29), 6.09 (1H, dd, $^3J_{H19\text{-}H20}$=7.5 Hz, H-19), 5.08 (1H, d, $^3J_{H25\text{-}H26}$=11.0Hz, H-25), 5.03 (1H, d, $^3J_{H21\text{-}HO}$=3.1 Hz, OH-21), 4.91 (1H, ddH-28), 4.38 (1H, d, ^2J=12.3 Hz, H-38a), 3.98 (1H, d, $^3J_{H23\text{-}HO}$=8.1 Hz, OH-23), 3.73 (1H, d, H-38b), 3.69 (1H, m, H-21), 3.28 (1H, m, H-39a), 3.23 (1H, d, $^3J_{H27\text{-}H28}$=8.6 Hz, H-27), 3.17 (1H, m, H-39b), 2.98 (2H, m, H-40), 2.89 (3H, s, H-37), 2.83 (1H, dd, $^3J_{H22\text{-}H23}$=8.8 Hz, $^3J_{H23\text{-}H24}$=9.1 Hz, H-23), 2.27 (1H, m, H-20), 1.98 (3H, s, H-36), 1.96 (3H, s, H-30), 1.92 (3H, s, H-14), 1.68 (1H, m, H-22), 1.65 (3H, s, H-13), 1.25 (1H, m, H-24), 0.97 (1H, m, H-26), 0.91 (3H, d, $^3J_{H22\text{-}H32}$=7.1 Hz, H-32), 0.85 (3H, d, $^3J_{H20\text{-}H31}$=6.9 Hz, H-31), 0.50 (3H, d, $^3J_{H24\text{-}H33}$=6.9 Hz, H-33), -0.33 (3H, d, $^3J_{H26\text{-}H34}$=6.8 Hz, H-34); ^{13}C NMR (δ ppm in DMSO-d_6): 185.3 (C-11), 184.2 (C-8), 171.8 (C-6), 170.2 (C-15), 169.4 (C-35), 160.6 (d, $^1J_{C\text{-}F}$=244.3 Hz, C-42), 148.9 (C-1), 145.0 (C-4), 143.1 (C-29), 139.1 (C-19), 131.6 (C-17), 131.4 (C-16), 131.1 (d, $^3J_{C\text{-}F}$=4.4 Hz, C-46), 129.2 (d, $^3J_{C\text{-}F}$=8.2 Hz, C-44), 126.2 (C-18), 124.8 (d, $^4J_{C\text{-}F}$=1.2 Hz, C-45), 123.7 (d, $^2J_{C\text{-}F}$=15.7 Hz, C-41), 118.0 (C-2), 117.7 (C-28), 116.7 (C-10), 115.4 (d, $^2J_{C\text{-}F}$=21.7 Hz, C-43), 115.1 (C-9), 114.8 (C-3), 108.8 (C-12), 101.4 (C-7), 98.6 (C-5), 76.3 (C-27), 75.8 (C-23), 73.2 (C-25), 72.8 (C-21), 55.7 (C-37), 46.8 (C-39), 43.1 (C-38), 40.3 (C-26), 38.2 (C-24), 37.9 (C-20), 32.7 (C-22), 25.2 (C-40), 22.1 (C-13), 20.7 (C-36), 19.8 (C-30), 18.2 (C-31), 11.2 (C-32), 9.0 (C-34), 8.8 (C-33), 7.4 (C-14); ^{15}N NMR (δ ppm in DMSO-d_6): -254 (N-2), -333 (N-38); ^{1}H, ^{13}C and ^{15}N resonance assignments were confirmed by COSY, HSQC, HMBC and NOESY 2D spectra; FT-IR (KBr pellet): 3447 and 3415 cm^{-1} $\nu(O_{21}\text{-}H) + \nu(O_{23}\text{-}H)$, 3337 cm^{-1} $\nu(N\text{-}H)_{amide}$, 3151 cm^{-1} $\nu(O_4\text{-}H\cdots O_{11})$, 2743 cm^{-1} $\nu(N_{38}{}^+\text{-}H\cdots O_{15})$, 2468 cm^{-1} $\nu(O_1\text{-}H\cdots O_8{}^-)$, 1724 cm^{-1} $\nu(C_{35}{=}O)$, 1646 cm^{-1} $\nu(C_{15}{=}O)_{amide\ I}$, 1597 cm^{-1} $\nu(C{=}C)_{naphthalene}$, 1561 cm^{-1} $\delta(N\text{-}H)_{amide\ II}$, 1544 cm^{-1} $\nu(C{=}C)$, 1457 and 1442 cm^{-1} $\nu(C{=}C)$, 1244 and 1235 cm^{-1} $\nu(C\text{-}O)$; Elemental analysis (%): Calcd. for $C_{46}H_{57}FN_2O_{12}$: C, 65.08; H, 6.77; N, 3.30; Found: C, 64.94; H, 6.71; N, 3.34.

Spectral data for (**12**): Yield 53% /method 3 with HCl(EtOH)/; m.p. 154-156°C; ESI-MS (*m/z*): 849 $[M+H]^+$; HR-MALDI-TOF 849.3968 $[M+H]^+$;^{1}H NMR (δ ppm in DMSO-d_6): 16.05 (1H, bs, OH-1), 12.84 (1H, s, OH-4), 9.30 (1H, s, NH_{amide}), 8.59 (1H, bs, $N^+H_{intramolecularly\ hydrogen\ bonded}$),

8.34 (1H, bs, $N^{+}H_{\text{hydrogen bonded with the solvent}}$), 7.36 (1H, m, H-45), 7.12 (1H, m, H-42), 7.09 (1H, m, H-46), 7.08 (1H, m, H-44), 6.60 (1H, dd, $^{3}J_{\text{H18-H19}}$=16.0 Hz, H-18), 6.33 (1H, d, $^{3}J_{\text{H17-H18}}$=11.0 Hz, H-17), 6.26 (1H, d, H-29), 6.09 (1H, dd, $^{3}J_{\text{H19-H20}}$=7.5 Hz, H-19), 5.09 (1H, d, $^{3}J_{\text{H25-H26}}$=11.0Hz, H-25), 5.03 (1H, d, $^{3}J_{\text{H21-HO}}$=3.1 Hz, OH-21), 4.94 (1H, dd, $^{3}J_{\text{H28-H29}}$=12.8 Hz, H-28), 4.25 (1H, d, ^{2}J=12.4 Hz, H-38a), 4.01 (1H, d, $^{3}J_{\text{H23-HO}}$=6.7 Hz, OH-23), 3.72 (1H, d, H-38b), 3.69 (1H, m, H-21), 3.34 (1H, m, H-39a), 3.24 (1H, d, $^{3}J_{\text{H27-H28}}$=8.4 Hz, H-27), 3.23 (1H, m, H-39b), 2.95 (2H, m, H-40), 2.90 (3H, s, H-37), 2.83 (1H, dd, $^{3}J_{\text{H22-H23}}$=8.8 Hz, $^{3}J_{\text{H23-H24}}$=9.1 Hz, H-23), 2.29 (1H, m, H-20), 1.98 (3H, s, H-36), 1.96 (3H, s, H-30), 1.93 (3H, s, H-14), 1.68 (1H, m, H-22), 1.65 (3H, s, H-13), 1.26 (1H, m, H-24), 0.99 (1H, m, H-26), 0.92 (3H, d, $^{3}J_{\text{H22-H32}}$=7.0 Hz, H-32), 0.87 (3H, d, $^{3}J_{\text{H20-H31}}$=7.0 Hz, H-31), 0.50 (3H, d, $^{3}J_{\text{H24-H33}}$=7.0 Hz, H-33), -0.32 (3H, d, $^{3}J_{\text{H26-H34}}$=6.8 Hz, H-34); ^{13}C NMR (δ ppm in DMSO-d_6): 185.3 (C-11), 184.1 (C-8), 171.8 (C-6), 170.3 (C-15), 169.4 (C-35), 162.3 (d, $^{1}J_{\text{C-F}}$=240.1 Hz, C-43), 148.9 (C-1), 145.0 (C-4), 143.0 (C-29), 139.8 (d, $^{3}J_{\text{C-F}}$=7.2 Hz, C-41), 139.1 (C-19), 131.6 (C-17), 131.4 (C-16), 130.5 (d, $^{3}J_{\text{C-F}}$=8.4 Hz, C-45), 126.2 (C-18), 124.8 (d, $^{4}J_{\text{C-F}}$=2.2 Hz, C-46), 118.0 (C-2), 117.7 (C-28), 116.6 (C-10), 115.5 (d, $^{2}J_{\text{C-F}}$=22.2 Hz, C-42), 115.1 (C-9), 114.6 (C-3), 113.6 (d, $^{2}J_{\text{C-F}}$=21.1 Hz, C-44), 108.8 (C-12), 101.3 (C-7), 98.5 (C-5), 76.3 (C-27), 75.8 (C-23), 73.2 (C-25), 72.8 (C-21), 55.6 (C-37), 47.6 (C-39), 43.0 (C-38), 40.3 (C-26), 38.1 (C-24), 37.9 (C-20), 32.7 (C-22), 31.3 (C-40), 22.0 (C-13), 20.6 (C-36), 19.8 (C-30), 18.2 (C-31), 11.2 (C-32), 8.9 (C-34), 8.7 (C-33), 7.3 (C-14); ^{15}N NMR (δ ppm in DMSO-d_6): -255 (N-2), -332 (N-38); ^{1}H, ^{13}C and ^{15}N resonance assignments were confirmed by COSY, HSQC, HMBC and NOESY 2D spectra; FT-IR (KBr pellet): 3442 and 3406 cm^{-1} $\nu(O_{21}\text{-H}) + \nu(O_{23}\text{-H})$, 3331 cm^{-1} $\nu(\text{N-H})_{\text{amide}}$, 3144 cm^{-1} $\nu(O_4\text{-H}\cdots O_{11})$, 2737 cm^{-1} $\nu(N_{38}\text{+-H}\cdots O_{15})$, 2472 cm^{-1} $\nu(O_1\text{-H}\cdots O_8^{-})$, 1720 cm^{-1} $\nu(C_{35}\text{=O})$, 1642 cm^{-1} $\nu(C_{15}\text{=O})_{\text{amide I}}$, 1599 cm^{-1} ν $(\text{C=C})_{\text{naphthalene}}$, 1555 cm^{-1} δ $(\text{N-H})_{\text{amide II}}$, 1541 cm^{-1} ν(C=C), 1453 and 1440 cm^{-1} ν(C=C), 1247 and 1239 cm^{-1} ν(C-O); Elemental analysis (%): Calcd. for $C_{46}H_{57}FN_2O_{12}$: C, 65.08; H, 6.77; N, 3.30; Found: C, 64.99; H, 6.71; N, 3.26.

Spectral data for (**13**): Yield 58% /method 3 with HCl(EtOH)/; m.p. 157-158°C; ESI-MS (*m/z*): 849 $[M+H]^{+}$; HR-MALDI-TOF 849.3979 $[M+H]^{+}$;^{1}H NMR (δ ppm in DMSO-d_6): 16.04 (1H, bs, OH-1), 12.84 (1H, s, OH-4), 9.31 (1H, s, NH_{amide}), 8.33 (1H, bs, $N^{+}H_{\text{intramolecularly hydrogen bonded}}$), 8.26 (1H, bs, $N^{+}H_{\text{hydrogen bonded with the solvent}}$), 7.28 (1H, dd, $^{3}J_{\text{H42/46-F}}$=5.7 Hz, $^{3}J_{\text{H42-H43/H45-H46}}$=8.3 Hz, H-42+H-46), 7.14 (1H, dd, $^{3}J_{\text{H43/H45-F}}$=8.8 Hz, H-43+H-45), 6.60 (1H, dd, $^{3}J_{\text{H18-H19}}$=15.9 Hz, H-18), 6.34 (1H, d, $^{3}J_{\text{H17-H18}}$=11.0 Hz, H-17), 6.26 (1H, d, $^{3}J_{\text{H28-H29}}$=12.9 Hz, H-29), 6.09 (1H, dd,

$^{3}J_{H19\text{-}H20}$=7.5 Hz, H-19), 5.09 (1H, d, $^{3}J_{H25\text{-}H26}$=11.0 Hz, H-25), 5.03 (1H, d, $^{3}J_{H21\text{-}HO}$=3.1 Hz, OH-21), 4.93 (1H, dd, H-28), 4.35 (1H, m, H-38a), 3.95 (1H, d, $^{3}J_{H23\text{-}HO}$=6.8 Hz, OH-23), 3.71 (1H, m, H-38b), 3.70 (1H, m, H-21), 3.29 (1H, m, H-39a), 3.25 (1H, d, $^{3}J_{H27\text{-}H28}$=8.7 Hz, H-27), 3.19 (1H, m, H-49b), 2.92 (2H, m, H-40), 2.90 (3H, s, H-37), 2.84 (1H, m, H-23), 2.29 (1H, m, H-20), 1.99 (3H, s, H-36), 1.97 (3H, s, H-30), 1.93 (3H, s, H-14), 1.69 (1H, m, H-22), 1.66 (3H, s, H-13), 1.27 (1H, m, H-24), 1.00 (1H, m, H-26), 0.92 (3H, d, $^{3}J_{H22\text{-}H32}$=7.2 Hz, H-32), 0.86 (3H, d, $^{3}J_{H20\text{-}H31}$=6.8 Hz, H-31), 0.51 (3H, d, $^{3}J_{H24\text{-}H33}$=7.0 Hz, H-33), -0.32 (3H, d, $^{3}J_{H26\text{-}H34}$=6.8 Hz, H-34); ^{13}C NMR (δ ppm in DMSO-d_6): 185.4 (C-11), 184.2 (C-8), 171.9 (C-6), 170.4 (C-15), 169.5 (C-35), 161.3 (d, $^{2}J_{C\text{-}F}$=242.8 Hz, C-44), 149.0 (C-1), 145.1 (C-4), 143.1 (C-29), 139.3 (C-19), 133.2 (d, $^{4}J_{C\text{-}F}$=1.2 Hz, C-41), 131.7 (C-17), 131.5 (C-16), 130.6 (d, $^{3}J_{C\text{-}F}$=8.4 Hz, C-42 + C-46), 126.3 (C-18), 118.1 (C-2), 117.8 (C-28), 116.7 (C-10), 115.5 (d, $^{2}J_{C\text{-}F}$=19.0 Hz, C-43 + C-45), 115.2 (C-9), 114.7 (C-3), 108.9 (C-12), 101.4 (C-7), 98.6 (C-5), 76.4 (C-27), 75.9 (C-23), 73.3 (C-25), 73.0 (C-21), 55.7 (C-37), 45.1 (C-39), 43.1 (C-38), 40.4 (C-26), 38.2 (C-24), 37.9 (C-20), 32.7 (C-22), 30.9 (C-40), 22.5 (C-13), 20.7 (C-36), 19.9 (C-30), 18.2 (C-31), 11.2 (C-32), 9.0 (C-34), 8.8 (C-33), 7.4 (C-14); ^{15}N NMR (δ ppm in DMSO-d_6): -254 (N-2), -333 (N-38); ^{1}H, ^{13}C and ^{15}N resonance assignments were confirmed by COSY, HSQC, HMBC and NOESY 2D spectra; FT-IR (KBr pellet): 3436 and 3999 cm^{-1} ν(O_{21}-H) + ν(O_{23}-H), 3331 cm^{-1} ν(N-H)$_{amide}$, 3138 cm^{-1} ν(O_4-H···O11), 2732 cm^{-1} ν(N_{38}^{+}-H···O15), 2464 cm^{-1} ν(O_1-H···O8^{-}), 1719 cm^{-1} ν(C_{35}=O), 1637 cm^{-1} ν(C_{15}=O)$_{amide\ I}$, 1596 cm^{-1} ν(C=C)$_{naphthalene}$, 1551 cm^{-1} δ(N-H)$_{amide\ II}$, 1538 cm^{-1} ν(C=C), 1448 i 1436 cm^{-1} ν(C=C), 1243 i 1239 cm^{-1} ν(C-O); Elemental analysis (%): Calcd. for $C_{46}H_{57}FN_2O_{12}$: C, 65.08; H, 6.77; N, 3.30; Found: C, 65.16; H, 6.69; N, 3.13.

Yield of **2-13** is given after column chromatography purification.

Antibacterial assays of 1 and 3-13

The antibacterial activity of the compounds studied was performed for a series of Gram-positive and Gram-negative bacteria, including the reference and hospital strains. The following microorganisms were used in this study: standard strains of Gram-positive cocci: *Staphylococcus aureus* NCTC 4163, *Staphylococcus aureus* ATCC 25923, *Staphylococcus aureus* ATCC 6538, *Staphylococcus aureus* ATCC 29213, *Staphylococcus epidermidis* ATCC 12228 and *Staphylococcus epidermidis* ATCC 35984; standard strains of Gram-negative rods: *Escherichia coli* ATCC 10538, *Escherichia coli* ATCC 25922, *Escherichia coli* NCTC 8196, *P. aeruginosa*

ATCC 15442, *P. aeruginosa* NCTC 6749, *P. aeruginosa* ATCC 27853. The microorganisms used were obtained from the collection of the Department of Pharmaceutical Microbiology, Medical University of Warsaw, Poland. Minimal Inhibitory Concentration (MIC) was determined by the twofold serial dilution method using Mueller-Hinton II agar medium (Beckton Dickinson) according to CLSI guidelines.[a] Concentrated solutions of the compounds tested in DMSO were made, then they were diluted in water to obtain the required concentration. The concentrations of the agents tested in a solid medium ranged from 8 to 0.002 μg mL^{-1} (for Gram-positive bacteria) and from 256 to 8 μg mL^{-1} (for Gram-negative bacteria). The final inoculum of all studied organisms were 104 CFU mL^{-1} (colony forming units per ml). Minimal inhibitory concentrations were read after 18h of incubation at 35 °C.

[a]Clinical and Laboratory Standards Institute Methods for Dilution Antimicrobial Susceptibility Tests for Bacteria That Grow Aerobically; Approved Standard M7-A-7, Clinical and Laboratory Standards Institute, Wayne, Pa. USA, 2006. The complete data of antibacterial tests were collected in Table 2.

Acknowledgement

The project was financially supported by Polish National Science Center (NCN), decision number DEC-2011/03/B/ST5/01014.

References

1 (*a*) H. G. Floss, T.-W. Yu, *Chem. Rev.* 2005, **105**, 621; (*b*) J. Mulzer, K. Schein, J. W. Bats, J. Buschmann, P. Luger, *Angew. Chem. – Int. Ed.* 1998, **37**, 1566.

2 (*a*) R. Cassano, S. Trombino, T. Ferrarelli, M. V. Mauro, C. Giraldi, M. Manconi, A. M. Fadda, N. J. Picci, *Biomed. Mat. Res. - Part A* 2012, **100A**, 536; (*b*) H. Syre, H. J. Grewal, *Antimicrob. Chemother.* 2011, **66**, 687; (*c*) T. Padayachee, K. P. Klugman, *Antimicrob. Agents Chemother.* 1999, **43**, 2361; (*d*) H. Bhutani, S. Saranjit, K. C. Jindal, A. K. Chakraborti, *J. Pharm. Biomed. Analys.* 2005, **39**, 892.

3 (*a*) N. Morisaki, Y. Hashimoto, K. Furihata, T. Imai, K. Watanabe, Y. Mikami, K. Yazawa, A. Ando, Y. Nagata, E. R. Dabbs, *J. Antibiot.* 2000, **53**, 269; (*b*) K. Yazawa, Y. Mikami, M. Maeda, M. Akao, N. Morisaki, S. Iwasaki, *Antimicrob. Agents Chemother.*

1993, **37**, 1313; (*c*) S. Ramaswamy, *J. M. Musser Tuberc. Lung Dis.* 1998, **79**, 3; (*d*) R. Figueiredo, D. F. Ramos, C. Moiteiro, M. A. Medeiros, M. J. Marcelo Curto, J. Cardoso De Menezes, R. H. Pando, P. E. A. Silva, M. D. C. Costa, *Eur. J. Med. Chem.* 2012, **47**, 186; (*e*) J. Li, Z. Ma, K. Chapo, D. Yan, A. S. Lynch, C. Z. Ding, *Bioorg. Med. Chem. Lett.* 2007, **17**, 5510.

4 W. Schulz, W. Zilling, *Nucleic Acid Res.* 1981, **9**, 6889.

5 E. A.Campbell, N. Korzheva, A. Mustaev, K. Murakami, S. Nair, A. Goldfarb, S. A. Darst, *Cell* 2001, **104**, 901.

6 A. Bacchi, G. J. Pelizzi, *Med. Chem.* 1998, **41**, 2319.

7 (*a*) R. Cricchio, G. Tamborini, P. Bravo, G. Gaudiano, *Il Farmaco Ed. Sc.* 1974, **29**, 358; (*b*) R. Cricchio, G. Lancini, G. Tamborini, P. Sensi, *J. Med. Chem.* 1974, **17**, 396; (*c*) R. Cricchio, G. Cietto, E. Rossi, V. Arioli, *Il Farmaco Ed. Sc.* 1975, **30**, 697; (*d*) M. Taguchi, N. Aikawa, G. Tsukamoto, *Chem. Pharm. Bull.* 1984, **43**, 4388; (*e*) G. Tsukamoto, M. Taguchi, N. Aikawa, *Chem. Pharm. Bull.* 1980, **28**, 2309.

8 J. R. McCarthy, J. L. Moore, D. V. Wysong, *J. Med. Chem.* 1977, **20**, 1272.

9 K. Pyta, P. Przybylski, B. Wicher, M. Gdaniec, J. Stefańska, *Org. Biomol. Chem.* 2012, **10**, 2385.

10 B. Wicher, K. Pyta, P. Przybylski, E. Tykarska, M. Gdaniec, *Acta Crystallogr. Sect. C: Cryst. Struct. Commun.* 2012, **C68**, o209.

11 M. Gadret, M. Goursolle, J. M. Leger, *J. C. Colleter, Acta Crystallogr., Sect. B: Struct. Crystallogr. Cryst. Chem.* 1975, **31**, 1454.

12 E. A. Campbell, O. Pavlova, N. Zenkin, F. Leon, H. Irschik, R. Jansen, K. Severinov, S. A. Darst, *EMBO Journal* 2005, **24**, 674.

13 D. Sanz, R. M. Claramunt, M. Angeles Garcia, I. Alkorta, J. Elguero, *Tetrahedron* 2011, **67**, 4633.

14 W. B. Jennings, *Chem. Rev.* 1975, **75**, 307.

15 H. Yamaguchi, S. Nakanishi, N. Kihara, T. Takata, *Tetrahedron Lett.* 2001, **42**, 1699.

16 P. Przybylski, K. Pyta, J. Stefańska, M. Ratajczak-Sitarz, A. Katrusiak, A. Huczyński, B. Brzezinski, *Eur. J. Med. Chem.* 2009, **44**, 4393.

17 M. Heep, U. Rieger, D. Beck, N. Lehn, *Antimicrob. Agents Chemother.* 2000, **44**, 1075.

18 Y. A. Ovchinnikov, G. S. Monastyrskaya, V. V. Gubanov, S. O. Guryev, O. Y. Chertov, N. N. Modyanov, V. A. Grinkevich, I. A. Makarova, T. V. Marchenko, I. N. Polovnikova, V. M. Lipkin, E. D. Sverdlov, *Eur. J. Biochem.* 1981, **116**, 621.

19 Cache WorkSystem Pro version 7.5.0.85 UserGuide (WinMopac 2007).

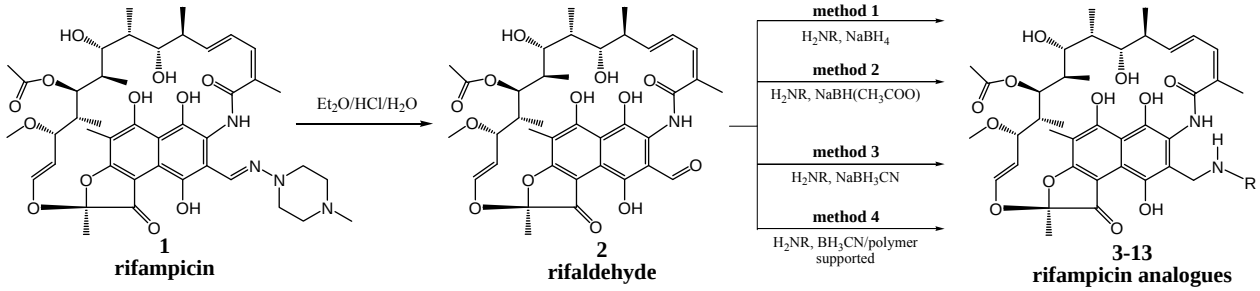

Figure 1 Methods for the synthesis of rifampicin halogen benzyl and phenethyl analogues.

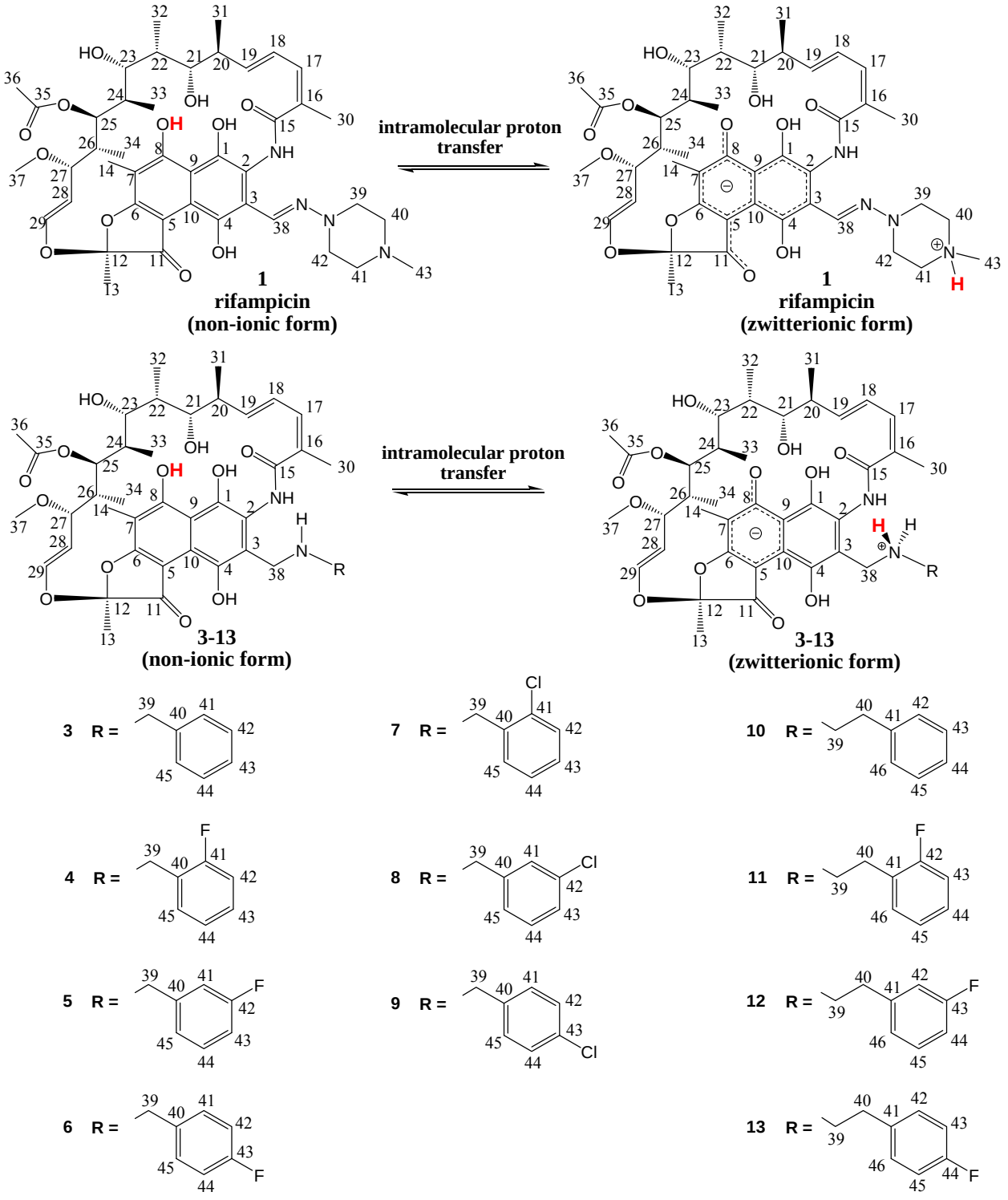

Figure 2 Intramolecular proton transfer realized in **1** and **3-13** compounds as well as their chemical structures together with the atom numbering.

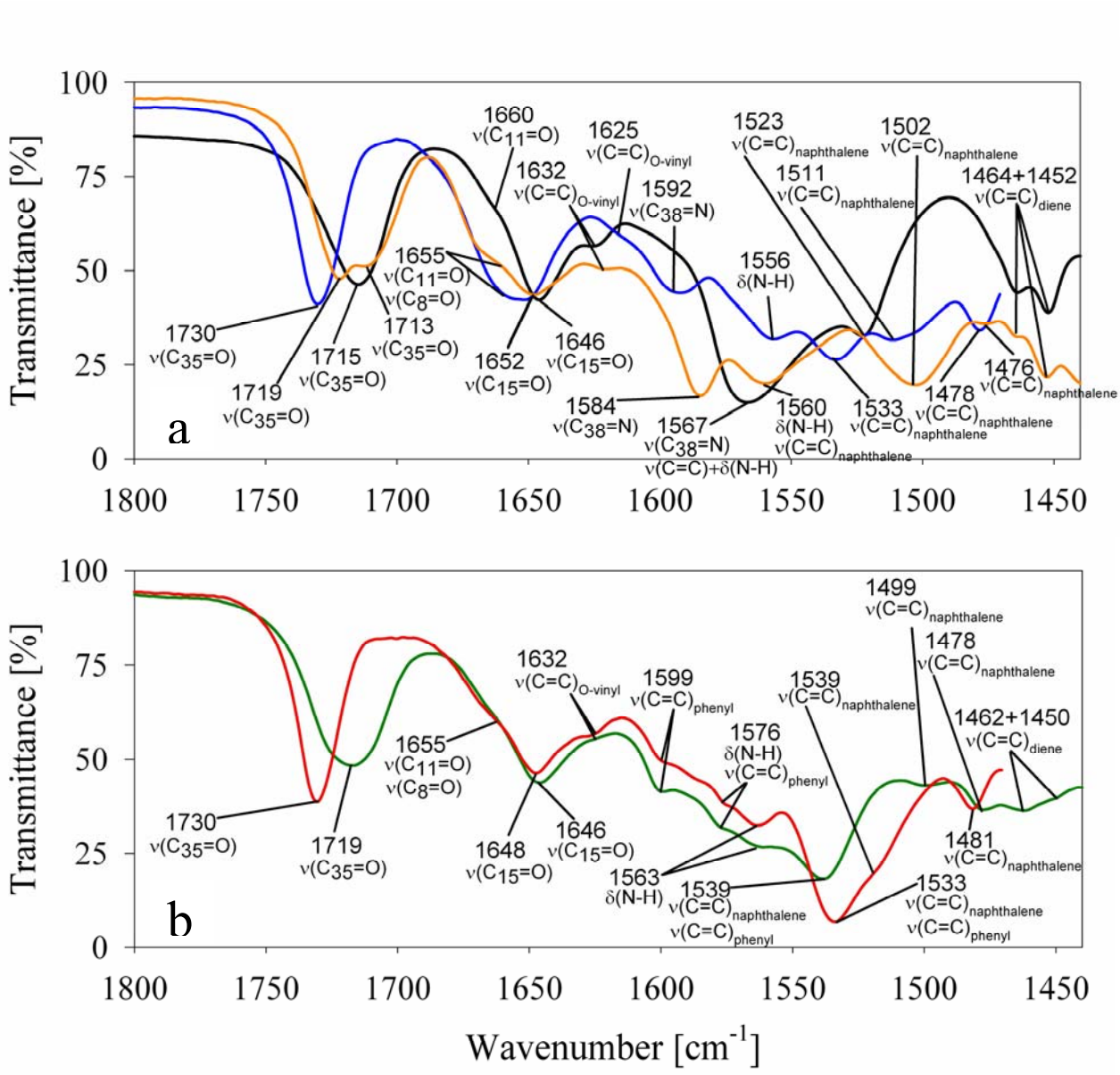

Figure 3 Comparison of FT-IR spectra in 1800-1450 cm^{-1} range: (a) (**black**) **1** in $CHCl_3$, (**blue**) **1** in DMSO/H_2O and (**orange**) 1:1 mixture of **1** with KOH in $CHCl_3$; (b) (**green**) **8** in $CHCl_3$ and (**red**) **8** in DMSO/H_2O.

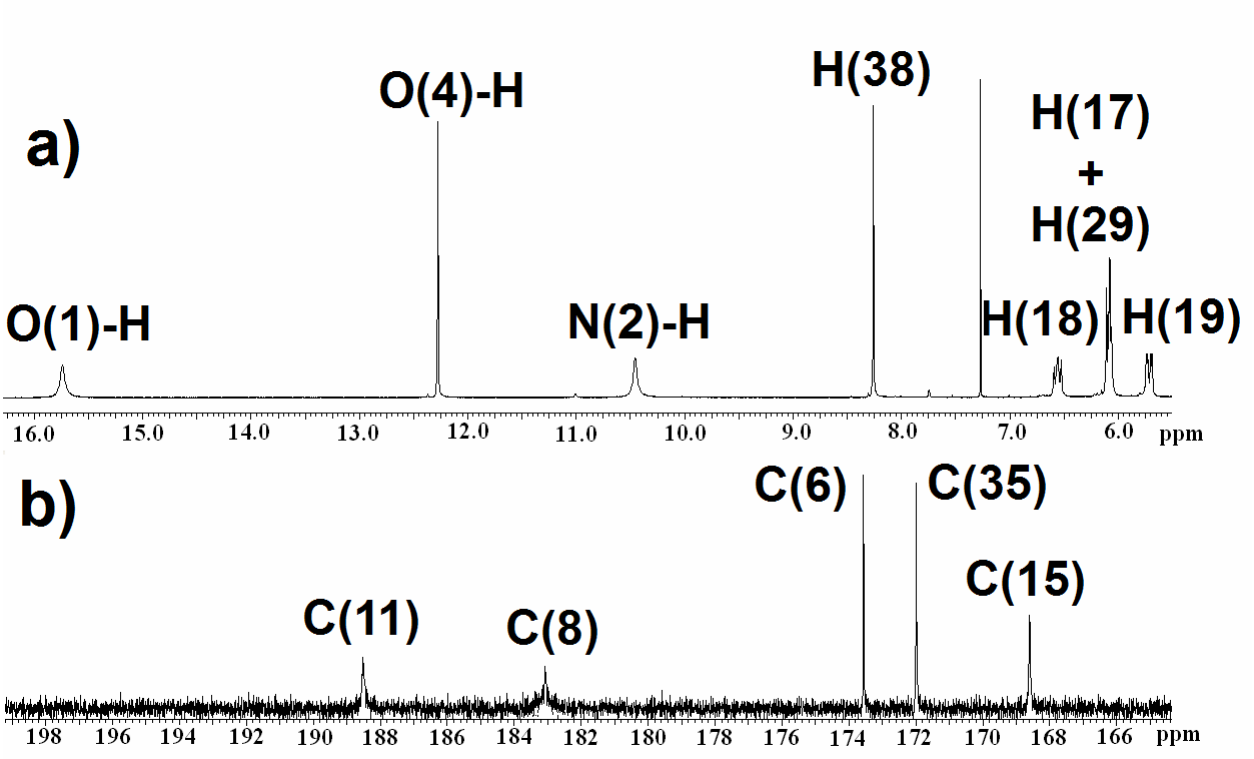

Figure 4 NMR spectra of deprotonated **1** (1:1 mixture of **1**-KOH): (a) ^{1}H NMR in the range 5.5-16 ppm and (b) ^{13}C NMR in the range 166-198 ppm, both recorded in $CDCl_3$.

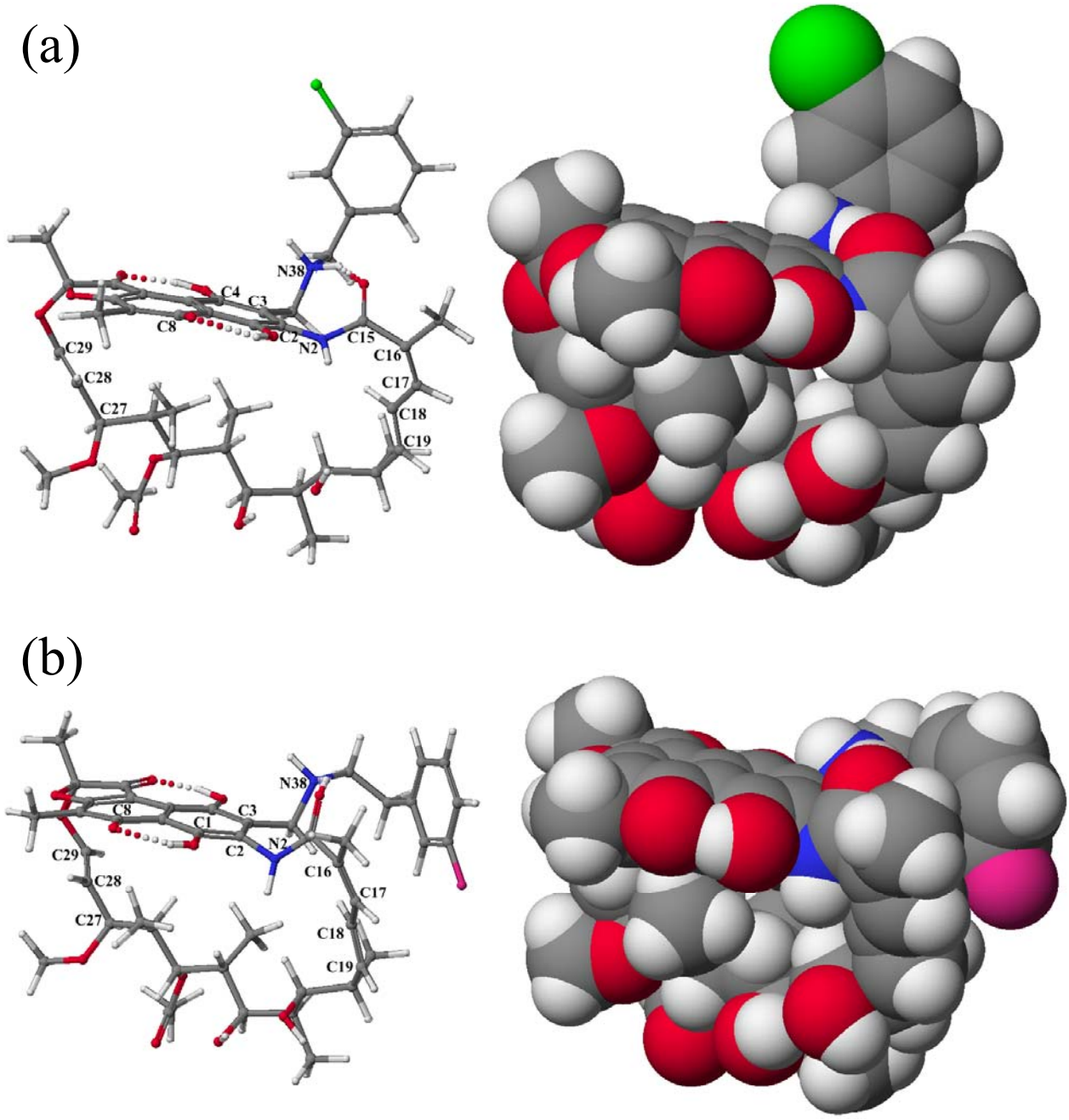

Figure 5 Stick and balls and space-filling projections of the most favourable structures showing different orientation of the substituent at C(3) atom for: (a) **8** ($H_f°$ = -457.5 kcal/mol), (b) **12** ($H_f°$ = -502.9 kcal/mol), calculated by PM5 method (WinMopac2007).

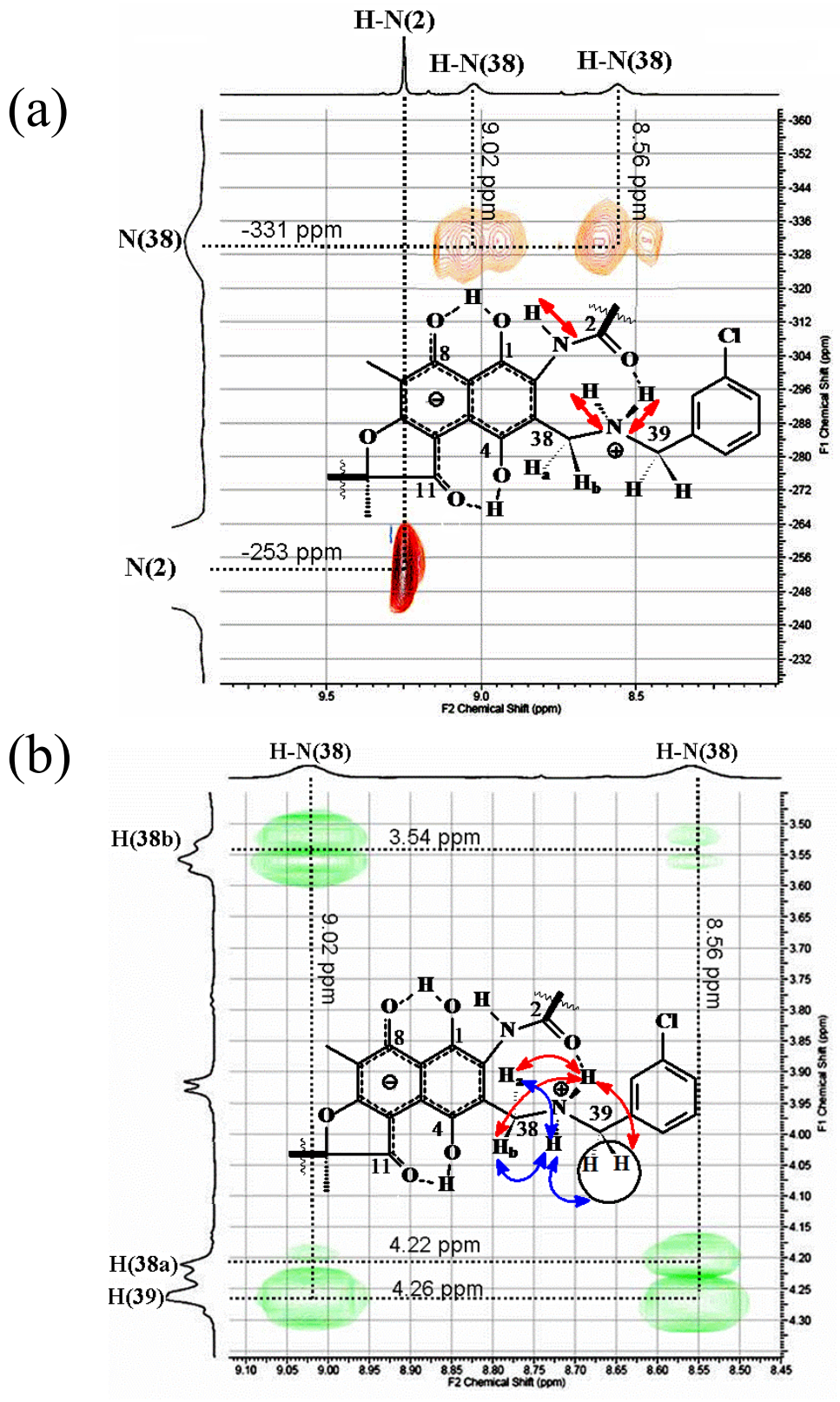

Figure 6 2D NMR spectra of **8** in DMSO-d_6+H_2O: (a) ^{1}H-^{15}N HSQC, (b) ^{1}H-^{1}H COSY.

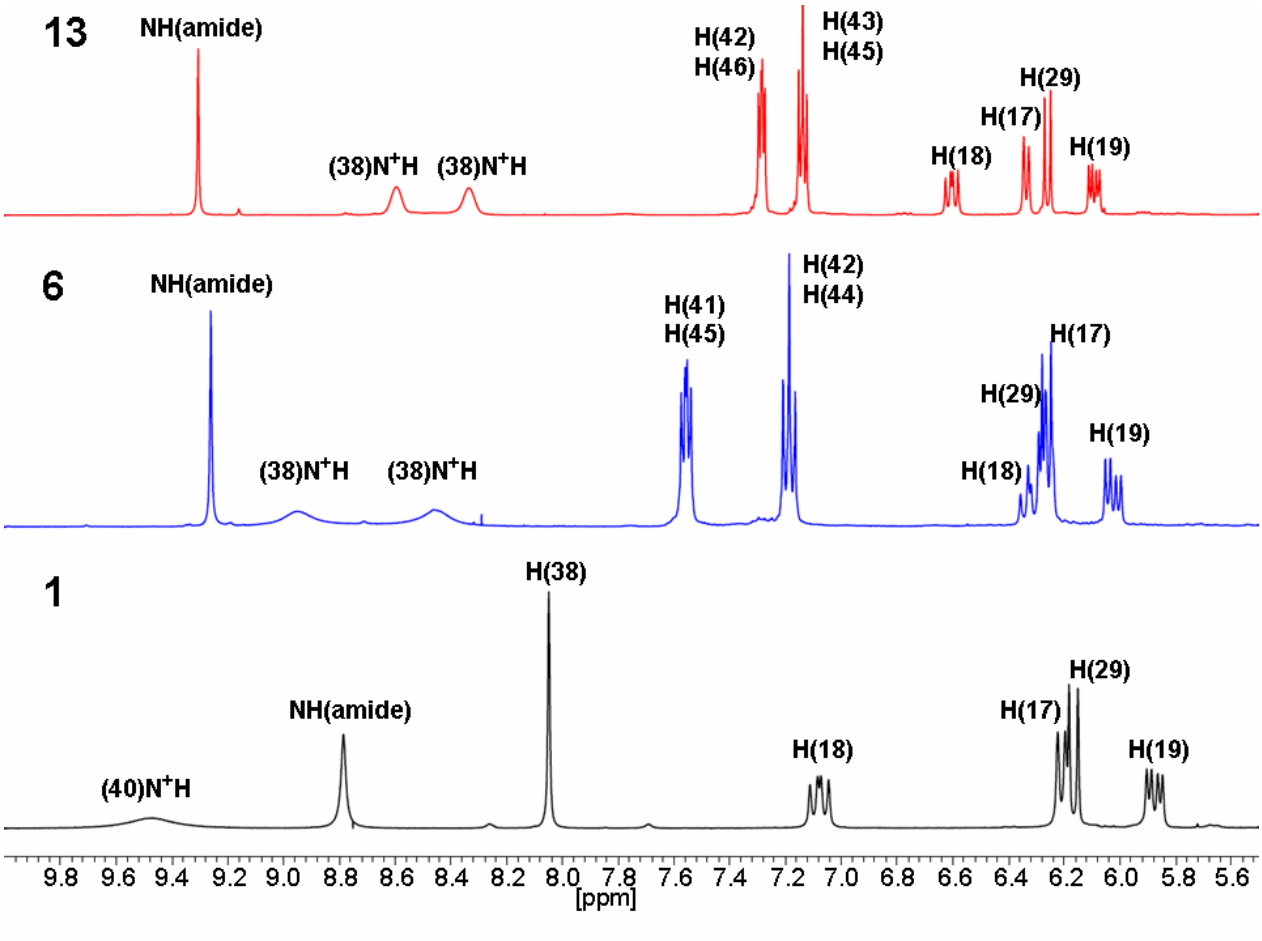

Figure 7 Comparison of ^{1}H NMR spectra of **1**, **6** and **13** (5.6-9.8 ppm range), recorded in DMSO-d_6/H_2O, demonstrating the difference in δ values of some protons from diene fragment of *ansa* chain (H-17, H-18).

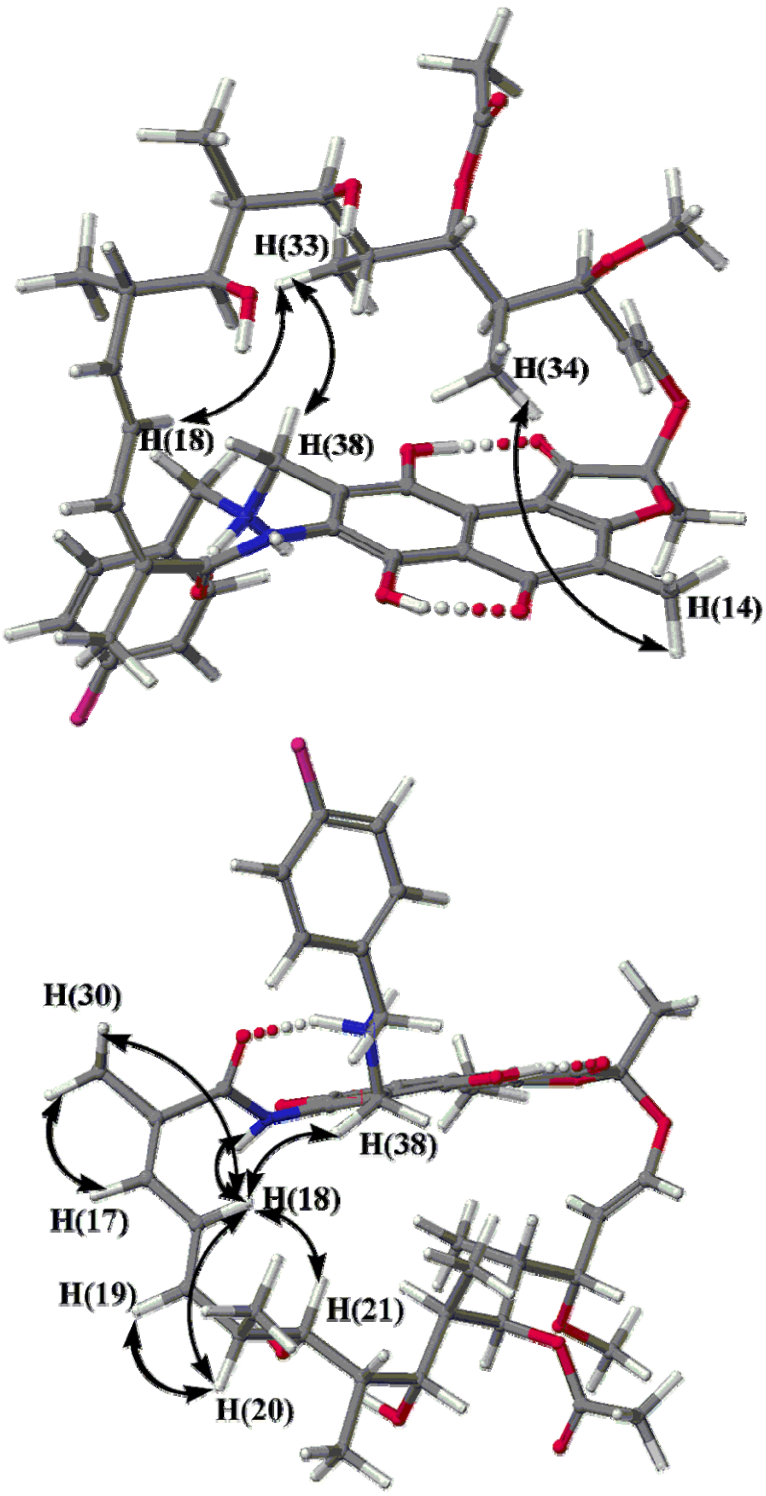

Figure 8 Selected proton-proton contacts determined from ^{1}H-^{1}H NOESY spectra for an exemplary rifampicin amino analogue (compound **13**). ^{1}H-^{1}H contacts were marked on energetically the most favourable structure /presented in the two projections/ calculated by PM5 method (WinMopac 2007).

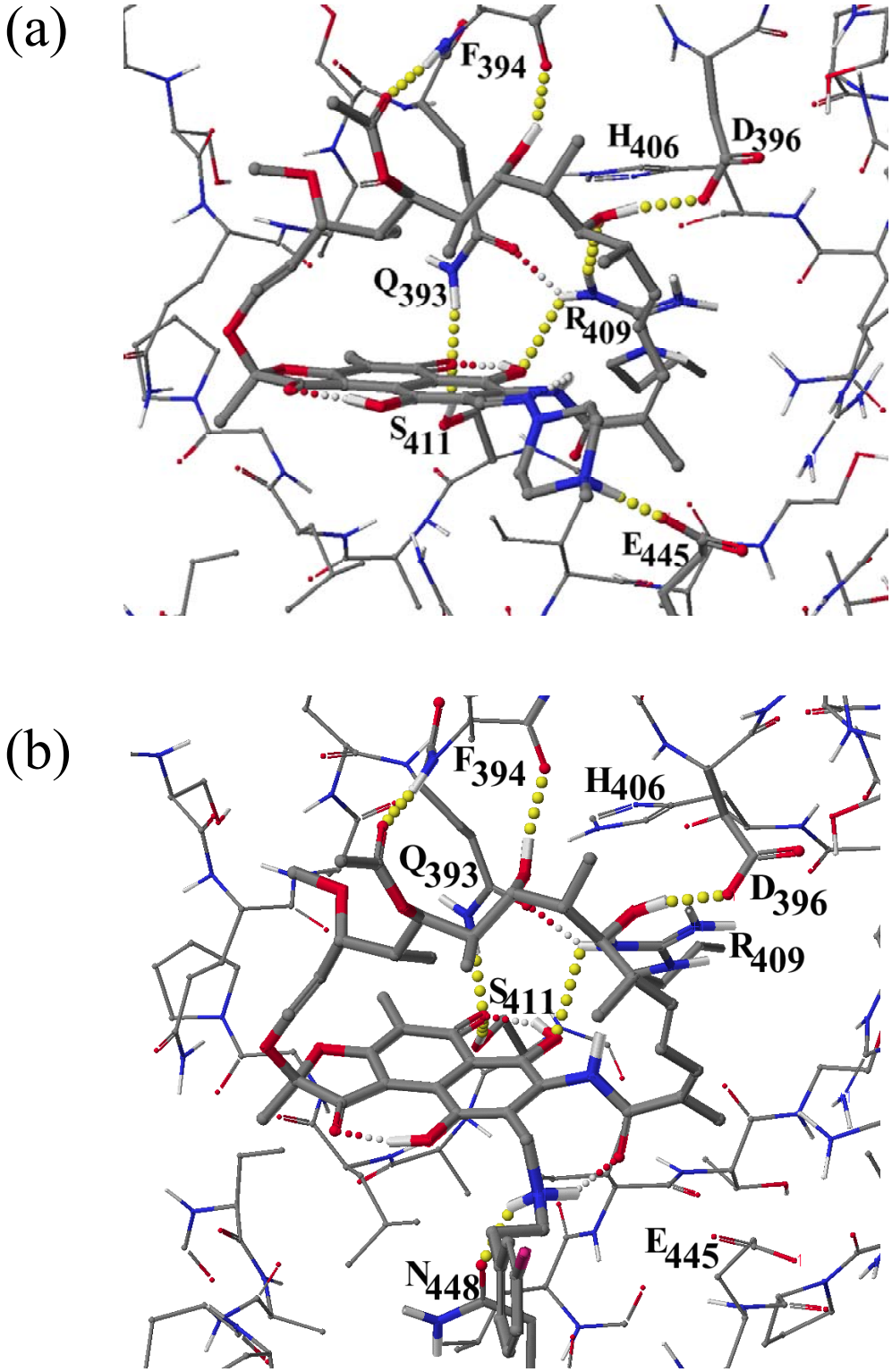

Figure 9 New model of the most energetically favourable interactions (marked by yellow) between aminoacid residues of RNAP and: (a) **1** (b) **12**; non-hydrogen bonded protons were omitted; calculated by PM5 method at semi-empirical level of theory (WinMopac2007), taking into account the zwitterionic forms of both inhibitor molecules as evidenced from spectroscopic studies in solution.

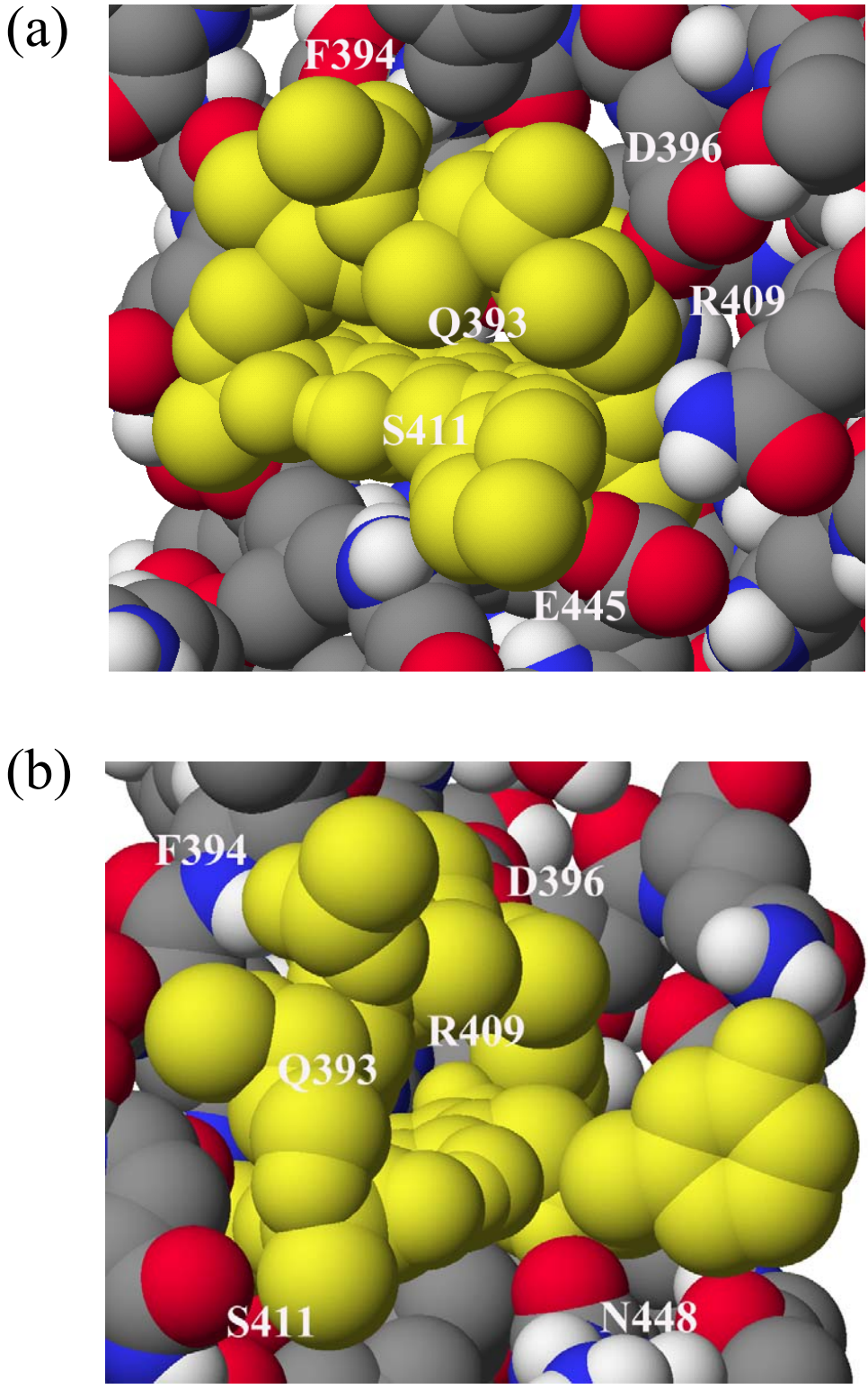

Figure 10 Space-filling projections of: (a) **1**-RNAP and (b) **12**-RNAP complexes, showing the spatial fit of the inhibitor (yellow) and the enzyme.

Table 1 Exemplary experimental data on reductive amination of **2** with *p*-chlorobenzylamine, performed *via* different methods with or without addition of catalyst.

Method	Catalyst / Reductant	Yield [%]*		
		without catalyst	$ZnCl_2$	HCl/EtOH
method 1	$NaBH_4$	<5	16	20
method 2	$NaBH(CH_3COO)_3$	40	59	70
method 3	$NaBH_3CN$	51	73	87
method 4	BH_3CN^-/ polymer supported	30	60	66

***** - calculated from ^{1}H NMR spectra *via* comparison of proton integral of amide [N(2)H, δ=9.24 ppm] with integral of internal standard (phthalimide) protons of aromatic ring [H-$C_{aromatic}$, δ=7.85 ppm]

Table 2 Antibacterial activity MIC (μg/ml) of new halogen benzyl (**3-9**) and phenethyl (**10-13**) amino analogues of rifampicin against standard Gram-(+) and Gram-(-) strains.

Bacteria Strain \ Compound	**1**	**3**	**4**	**5**	**6**	**7**	**8**	**9**	**10**	**11**	**12**	**13**
S. aureus NCTC 4163	0.008	0.5	0.5	0.5	0.5	0.5	1	1	1	0.5	0.5	0.5
S. aureus ATCC 25923	0.016	1	2	2	1	1	4	4	2	1	2	2
S. aureus ATCC 6538	0.008	0.5	0.5	0.5	0.5	0.5	1	1	1	0.5	0.5	0.5
S. aureus ATCC 29213	0.008	0.5	0.5	1	0.5	0.5	1	1	1	0.5	0.5	1
S. epidermidis ATCC 12228	0.004	0.25	0.125	0.125	0.125	0.125	0.5	0.125	0.25	0.125	0.125	0.25
S. epidermidis ATCC 35984	0.016	0.25	0.25	0.5	0.25	0.125	1	0.5	0.5	0.25	0.25	0.5
E. coli ATCC 10538	16	>256	256	>256	256	>256	>256	>256	>256	>256	>256	>256
E. coli ATCC 25922	8	128	64	64	128	128	256	128	>256	>256	256	>256
E. coli NCTC 8196	8	128	64	64	128	128	256	128	>256	256	128	256
P. aeruginosa ATCC 15442	32	256	256	>256	256	>256	>256	>256	>256	>256	>256	256
P. aeruginosa NCTC 6749	16	>256	256	>256	256	256	>256	>256	>256	>256	256	256
P. aeruginosa ATCC 27853	16	256	128	256	128	256	>256	>256	>256	>256	256	>256

Table 3 Intermolecular hydrogen bonds in a new model of RNAP inhibition; [angle °; distance Å] between amino acid residues of enzyme part and **1** or **12** proton acceptor and proton donor atoms.

RNAP - 1	Interatomic distance [D···A] [Å]	Angle [D-H···A] [°]
(Q_{393}) N-H···O=C(8)	2.76	163
(F_{394}) N-H···O=C(35)	2.95	169
(F_{394}) C=O···H-O(23)	2.73	127
(D_{396}) C=O···H-O(21)	2.80	165
(H_{406}) N-H···O(23)	3.74	154
(R_{409}) N-H···O(1)	2.89	98
(R_{409}) N-H···O(21)	3.48	165
(S_{411}) O-H···O=C(8)	2.80	167
(E_{445}) C=O···H-N^{+}(40)	2.57	176
RNAP - 12		
(Q_{393}) N-H···O=C(8)	2.78	164
(F_{394}) N-H···O=C(35)	2.90	153
(F_{394}) C=O···H-O(23)	2.84	160
(D_{396}) C=O···H-O(21)	2.76	164
(H_{406}) N-H···O(23)	3.91	156
(R_{409}) N-H···O(1)	2.96	100
(R_{409}) N-H···O(21)	3.93	159
(S_{411}) O-H···O=C(8)	2.80	170
(N_{448}) C=O ···H-N^{+}(38)	2.73	140

D - donor atom in hydrogen bond, A – acceptor atom in hydrogen bond